The Aryl Hydrocarbon Receptor is a Critical Regulator of Tissue Factor Stability and an Antithrombotic Target in Uremia

Sowmya Shivanna,* Kumaran Kolandaivelu,† Moshe Shashar,* Mostafa Belghasim,‡ Laith Al-Rabadi,* Mercedes Balcells,†§ Anqi Zhang,‖ Janice Weinberg,¶ Jean Francis,* Michael P. Pollastri,** Elazer R. Edelman,† David H. Sherr,†† and Vipul C. Chitalia*

*Renal Section, Department of Medicine, Boston University School of Medicine, Boston, Massachusetts; †Institute of Medical Engineering and Science, Massachusetts Institute of Technology, Cambridge, Massachusetts; ‡Department of Pathology and Laboratory Medicine, Boston University School of Medicine, Boston, Massachusetts; §Biological Engineering Department, Institut Químic de Sarrià, Ramon Llull University, Barcelona, Spain; ‖Metabolomics Core, Department of Medicine, Boston University School of Medicine, Boston, Massachusetts; ¶Department of Biostatistics, School of Public Health, Boston University, Boston, Massachusetts; **Department of Chemistry and Chemical Biology, Northeastern University, Boston, Massachusetts; and ††Department of Environmental Health, Boston University School of Public Health, Boston University School of Medicine, Boston, Massachusetts

ABSTRACT

Patients with CKD suffer high rates of thrombosis, particularly after endovascular interventions, yet few options are available to improve management and reduce thrombotic risk. We recently demonstrated that indoxyl sulfate (IS) is a potent CKD-specific prothrombotic metabolite that induces tissue factor (TF) in vascular smooth muscle cells (vSMCs), although the precise mechanism and treatment implications remain unclear. Because IS is an agonist of the aryl hydrocarbon receptor (AHR), we first examined the relationship between IS levels and AHR-inducing activity in sera of patients with ESRD. IS levels correlated significantly with both vSMC AHR activity and TF activity. Mechanistically, we demonstrated that IS activates the AHR pathway in primary human aortic vSMCs, and further, that AHR interacts directly with and stabilizes functional TF. Antagonists directly targeting AHR enhanced TF ubiquitination and degradation and suppressed thrombosis in a postinterventional model of CKD and endovascular injury. Furthermore, AHR antagonists inhibited TF in a manner dependent on circulating IS levels. In conclusion, we demonstrated that IS regulates TF stability through AHR signaling and uncovered AHR as an antithrombotic target and AHR antagonists as a novel class of antithrombotics. Together, IS and AHR have potential as uremia-specific biomarkers and targets that may be leveraged as a promising theranostic platform to better manage the elevated thrombosis rates in patients with CKD.

J Am Soc Nephrol 27: 189–201, 2016. doi: 10.1681/ASN.2014121241

CKD creates a highly thrombogenic milieu[1,2] and represents a potent risk factor for both venous thromboembolic events and arterial thrombosis manifesting as endovascular thrombosis following angioplasty, coronary stenting, and arteriovenous fistula interventions. Clinical trials demonstrate that CKD independently increases the risk of coronary stent thrombosis by 6.5–10-fold, a risk factor second in impact to inadequate antithrombotic medications, strongly implicating renal failure–specific prothrombotic mediators.[3,4] Beyond disease-specific propensities alone, thrombosis management in CKD patients poses unique challenges. While conventional antithrombotic medications have reduced effectiveness in CKD patients,

Received December 19, 2014. Accepted April 11, 2015.

Published online ahead of print. Publication date available at www.jasn.org.

Correspondence: Dr. Vipul Chitalia, Renal Section, Department of Medicine, Boston University Medical Center, Evans Biomedical Research Center, X-530, Boston, MA 02118. Email: vichital@bu.edu

bleeding risk is simultaneously increased leading to a narrow therapeutic window.[5–7] Identifying CKD-specific therapeutic targets is a promising strategy for reducing CKD-related thrombotic complications.

The state of the local vessel wall drives postinterventional thrombogenicity. Endothelial cell (EC) denudation exposes vascular smooth muscle cells (vSMCs) and thrombogenic constituents. Notably, tissue factor (TF), the initiator of extrinsic coagulation, is highly expressed in vSMCs.[8,9] In renal failure, uremic metabolite accumulation can inflict direct cellular stresses.[10,11] In particular, the indolic metabolites, indoxyl sulfate (IS) and indoxyl acetate (IA), were recently implicated in postinterventional thrombosis through enhancement of vSMC TF by inhibiting TF ubiquitination and degradation.[8] As mechanisms through which IS and IA mediate these effects were poorly characterized, it remained unclear how to leverage these findings to develop CKD-specific therapeutics.

We now demonstrate the critical role for the aryl hydrocarbon receptor (AHR) in uremic thrombosis. The AHR is a highly conserved receptor/transcription factor with important roles in xenobiotic metabolism, carcinogenicity, and vascular inflammation.[12,13] In addition to its transcriptional roles, it mediates degradation of proteins through the ubiquitin ligase complex.[14,15] Several endogenous chemicals, including IS, bind to and activate the AHR.[12,16] Therefore, we hypothesized that IS accumulation in CKD patients induces TF through an AHR pathway, thus potentiating thrombosis. Our results demonstrate that the AHR regulates baseline and IS-mediated vSMC TF levels and activity and show the feasibility of targeting this AHR pathway with novel competitive AHR antagonists able to modify CKD-specific thrombotic risk.

RESULTS

Patient Characteristics

Sera were obtained with patient consent and approval of the institutional review boards of both the Boston University Medical Campus and the Massachusetts Institute of Technology from 20 patients with ESRD receiving maintenance hemodialysis. Baseline characteristics (Supplemental Table 1) describe a cohort representative of Boston's inner city population comprising 17 black and three Hispanic patients, predominantly males, with median age 49 years (range 27–43 years) and relatively high body mass index (median 26.5, range 17–41).[8] Diabetes and hypertension were dominant causes of ESRD. Vascular disease (cardiovascular, cerebrovascular, and peripheral vascular diseases) was present in 35%–40% of patients. Half were taking 81 mg/day of aspirin; none were taking anticoagulants.

IS Correlates with AHR and TF Activities in ESRD Patients

Our previous work examined the overall effect of uremia and showed that IS or pooled uremic sera increased TF expression and activity in vSMCs.[8] We now demonstrate patient-specific IS levels (liquid chromatography/mass spectrometry; Supplemental Figure 1, Supplemental Tables 2 and 3) correlate with quantitative vSMC TF function and further validate this relationship using age, gender, and ethnicity-matched controls. ESRD patients had, on average, a 55-fold higher level of IS than controls ($P<0.001$) (Table 1). Similarly, vSMC procoagulant TF activity (Supplemental Figure 2) increased following exposure to sera from individual ESRD patients ($P<0.001$), correlating significantly with IS level in individual ESRD patients (Spearman correlation coefficient=0.71, $P<0.001$) (Table 2).

As IS is a known AHR agonist,[16] and human medium-sized blood vessels show high expression of AHR in vSMCs (Figure 1A, Supplemental Figure 3), we posited that IS levels are likely to correlate with AHR activity, as measured using a promoter-reporter assay (Supplemental Figure 4). Compared with controls, AHR activity was significantly higher in uremic patients ($P<0.001$), and in addition to IS levels (Spearman correlation

Table 1. Levels of IS, AHR activity, and procoagulant TF activity in pairs of ESRD patients and age, gender, and ethnicity-matched controls

Pair	IS μg/ml		AHR Activity		TF Activity (pM)	
	Control	Uremic	Control	Uremic	Control	Uremic
1	2.29	54.30	1.31	5.55	213.29	262.41
2	0.65	21.85[a]	1.82	4.21	206.62	271.90
3	1.30	48.85[a]	2.00	5.48	149.75	297.93
4	1.33	24.75	1.39	3.50	247.96	284.50
5	1.54	34.90	1.55	4.66	303.47	276.84
6	0.08	70.50	2.30	7.60	185.93	319.83
7	0.33	26.75	1.98	5.52	234.44	284.79
8	2.40	52.65	1.91	3.02	316.00	426.32
9	0.61	55.65[a]	1.71	6.75	206.04	412.57
10	1.30	66.45[a]	1.98	7.62	309.75	426.32
11	1.00	21.80	1.51	4.28	233.70	306.71
12	0.43	11.10[a]	1.49	3.62	286.43	276.63
13	1.39	58.40[a]	2.38	5.99	192.66	330.10
14	0.06	54.05	2.17	6.06	239.33	347.37
15	2.00	75.35[a]	1.10	6.10	187.47	493.88
16	1.05	43.25	1.75	4.37	230.79	306.10
17	0.85	73.25[a]	1.91	5.76	128.19	428.42
18	1.22	44.65	1.88	5.31	218.04	276.63
19	1.47	13.95	1.91	4.38	187.73	274.24
20	2.41	44.65	1.67	4.21	227.29	329.52
Mean	1.18	44.86	1.79	5.20	225.00	332.00
Median	1.26	46.75	1.85	5.40	223.00	306.00
SD	0.72	19.73	0.33	1.29	50.00	68.00
Range	0.059–2.4	11.1–75.35	1.1–2.38	3.02–7.62	128–316	262–494
P value[b]	<0.001		<0.001		<0.001	

[a]ESRD patients included in Figure 5E.
[b]Comparison of matched pairs using paired *t* test and Wilcoxon signed rank yielded the same results.

Table 2. Spearman Correlations (*P* values in parenthesis) by group

Group		AHR	TF
Uremic	IS	0.77 (<0.001)	0.71 (0.001)
	AHR		0.45 (0.05)
Control	IS	−0.37 (0.11)	0.09 (0.69)
	AHR		−0.20 (0.39)

coefficient=0.77, $P<0.001$), it significantly correlated with TF activity in individual ESRD patients (Spearman correlation coefficient=0.45, $P=0.05$, Table 2), raising an interesting possibility of AHR mediating IS-induced TF and an IS-AHR-TF thrombosis axis.

Diabetes is a strong risk factor for both CKD and thrombosis. It enhances thrombosis by perturbing several components of the coagulation system[17] raising the possibility of it being a confounder in the above cohort, which consisted of 45% diabetic patients. However, a subgroup analysis of control-matched nondiabetic ESRD patients revealed significantly higher IS levels and TF and AHR activities; also significant correlations between IS and AHR (Spearman correlation coefficient=0.62, $P=0.03$) and IS and TF (Spearman correlation coefficient=0.88, $P=0.004$) were found in the nondiabetic ESRD group (Supplemental Tables 5 and 6). Although these findings need validation in larger cohorts, it points to the independence of this axis from diabetes.

IS Activates AHR Signaling in vSMCs

We mechanistically examined the hypothesis that IS regulates TF through AHR signaling in vSMCs. Four events characterize AHR activation: (*1*) AHR nuclear translocation; (*2*) increased AHR transcriptional activity; (*3*) upregulation of prototypic target genes such as *CYP1B1*;[12] and (*4*) proteasomal AHR degradation as it cycles out of the nucleus.[12,13] In vSMCs, IS treatment induced each of these characteristics in a manner blocked by competitive AHR antagonists. vSMC baseline AHR was predominantly cytosolic as determined by western blotting (Figure 1B) and immunofluorescence (Figure 1C). A minor nuclear fraction indicated basal activation. Both IS and uremic serum induced AHR nuclear translocation within 20 minutes (Figure 1, B and C), an effect abrogated by a novel AHR antagonist, CB7993113, developed by our group[18] and CH223191, a well established AHR antagonist[19] (Figure 1C, Supplemental Figure 5).

Since IS circulates in albumin-bound and free forms,[10,11,20] we examined AHR activation with both forms using concentrations observed in different CKD stages (Supplemental Table 4). In an AHR-driven reporter assay, both IS forms induced dose-dependent AHR transcription. IS levels equivalent to those found in early CKD patients also significantly increased AHR activity, which was dose-dependently suppressed by CB7993113 (Figure 1D, Supplemental Figure 6, B and C). Similarly, IS increased expression of endogenous AHR-target genes *Cyp1a1*, *Cyp1b1*, *and Ahrr*, all of which were suppressed by AHR antagonist (Figure 1E). Downregulation of AHR expression in controls and even more so with uremic sera is consistent with AHR activation followed by proteasomal degradation[12,16] within 12 hours of treatment (Figure 1F). AHR levels remained stable with AHR antagonist, likely due to prevention of AHR activation and degradation.

AHR Signaling Mediates IS Regulation of TF

As IS activated AHR signaling in vSMCs (Figure 1), we posited that IS may regulate TF through AHR and examined this hypothesis via three models: (*1*) $AHR^{-/-}$ KO cells; (*2*) cells in which AHR is silenced; and (*3*) AHR antagonists.

Human vSMCs stably expressing a doxycycline-inducible short hairpin AHR construct showed substantially lowered AHR and TF levels after 48 hours (Figure 2A). Compared with mouse embryonic fibroblast (MEFs) from wild-type animals, $AHR^{-/-}$ mice[21] MEFs had barely detectable TF (Supplementary Figure 7A, Figure 2B). In contrast, $AHR^{-/-}$ cells, in which AHR expression was reestablished by gene knock-in (KI), expressed significant TF levels. Treatment with IS upregulated TF in AHR KI cells significantly more than $AHR^{-/-}$ mice. Both AHR antagonists significantly reduced the IS-induced or uremic serum–induced increase in TF expression and activity (Figure 2, C–F). Interestingly, CB7993113 reduced TF activity even in vSMCs incubated with sera from healthy volunteers (Figure 2, E and F), suggesting AHR regulating TF even with a baseline of AHR activity induced by endogenous ligands.[12,16] AHR antagonists suppressed IS-induced or uremic serum–induced TF levels significantly more (95% suppression) than they suppressed baseline TF levels (67% suppression, $P=0.03$) (Figure 2, C and E). No free levels of IS were examined in cells treated with albumin and IS. However, as only the free form of IS is deemed biologically active, the increase in both TF and AHR activities suggests the presence of sufficient levels of free IS in the milieu. Of note, other canonical AHR agonists, 6-formylindole[3,2-b]carbazole (FICZ) and β-naphtoflavone (β-NF), and an antagonist, 3′methoxy-4'nitroflavone (MNF), regulated TF according to their respective AHR activities (*i.e.*, agonists increased and the antagonists reduced TF), further strengthening the role of AHR as a regulator of TF (Supplementary Figure 7, B–D).

Several mediators can increase TF in vSMCs postinjury, *e.g.*, thrombin, TNFα, and CD40L.[9] IS further augments TF expression after vSMC injury,[8] which was reduced by CH223191 (Figure 2G) demonstrating the profound effect of AHR inhibition.

Since AHR regulates TF protein, we examined whether AHR and TF physically interact. Immunoprecipitation of TF resulted in coprecipitation of AHR and *vice versa* (Figure 3A). Since indirect protein interactions could not be excluded in *in vivo* co-IP studies, we used an *in vitro* binding assay using bacloviral purified human full-length, His-tagged AHR protein immobilized on nickel beads, and soluble bacloviral purified human TF. Purified AHR interacted with purified TF (Figure 3B). Immunofluorescence demonstrated predominantly cytosolic AHR with a portion in the nucleus whereas TF localized to the vSMCs cytosol and membrane (Figure 3C).

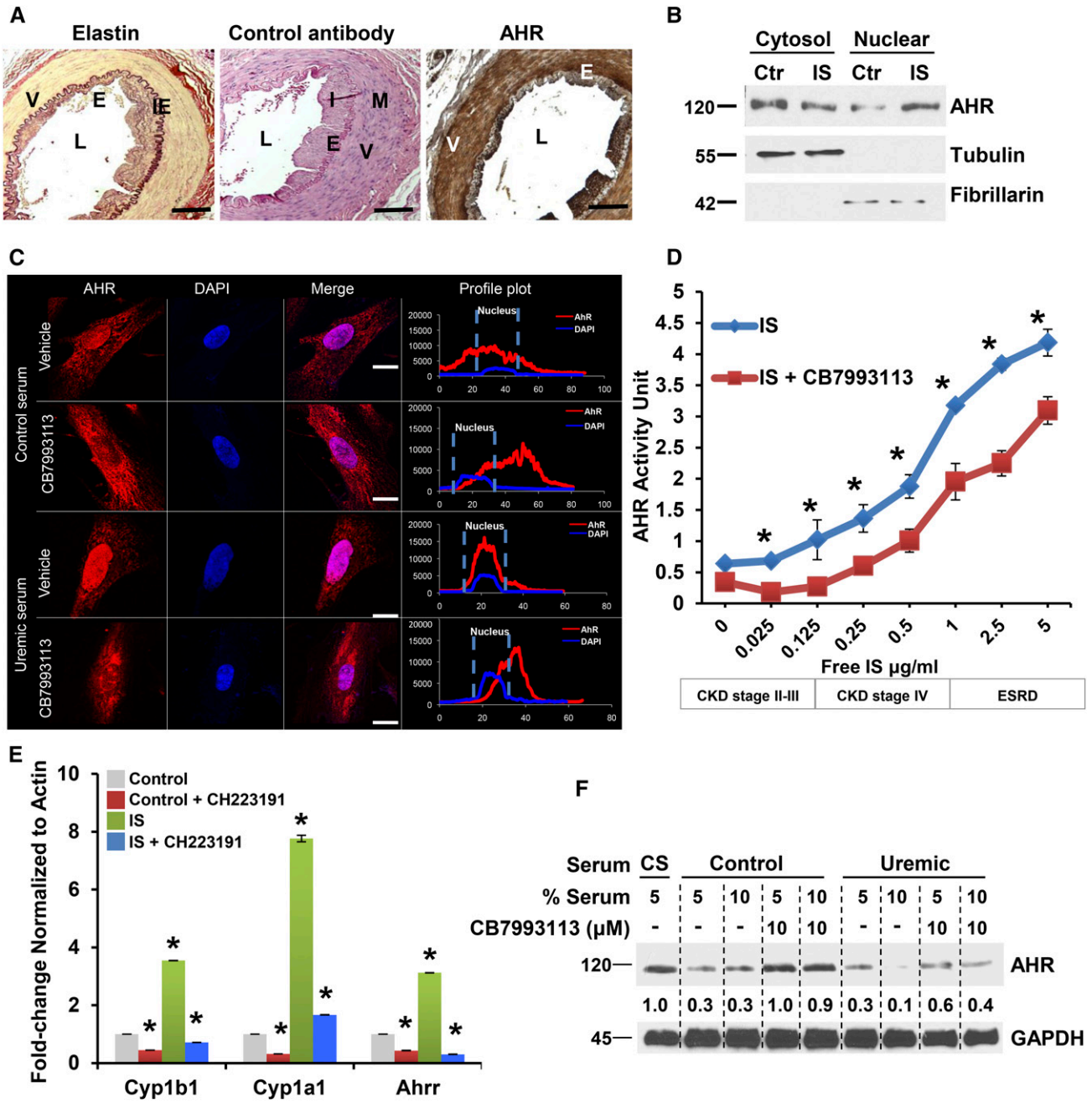

Figure 1. IS stimulates AHR signaling in vSMCs. (A) Expressions of AHR in vSMCs of normal human temporal artery. Paraffin-embedded sections of a temporal artery from a 63-year-old male stained with elastin stain or rabbit control antibody or AHR antibody along with hematoxylin and eosin are shown. Elastin stains internal and external elastic laminae. A representative image from eight independent human subjects is shown. L, lumen; I, intima; M, media; IE, internal elastic lamina; E, endothelial cells; V, vSMCs. Scale bar, 100 μM. (B) Nuclear translocation of AHR following activation by IS. Primary human aortic vSMCs were treated with control or IS (25 μg/ml), as described previously.[8] Subcellular fractionation was performed. Tubulin and fibrillarin (cytosol and nuclear markers, respectively) served as loading controls. A representative of three independent experiments is shown. (C) AHR antagonist abrogates uremic serum–induced nuclear translocation of AHR. Subconfluent serum-starved vSMCs treated with 5% pooled control and uremic sera and 10 μM CB7993113 for 20 minutes and subjected to immunofluorescence microscopy. Representative images from 150 randomly counted cells are shown. Profile plots were generated using ImageJ, which delineates the distribution and the signal intensity over the length of a cell. The broken line delineates the nucleus and nuclear AHR. Scale bar, 10 μM. (D) The free form of IS activates and AHR antagonism suppresses AHR activity in vSMCs. vSMCs stably expressing a xenobiotic responsive element promoter–luciferase reporter construct were treated with IS corresponding to different CKD stages (Supplemental Table 4) and AHR antagonist CB7993113 (10 μM) for 24 hours in serum-free medium. AHR activity was quantified by firefly luciferase units and converted to AHR activity unit using

Both colocalized in the perinuclear region. Colocalization, represented as a scatter plot with the pixel density of flurophore, is displayed along the entire Z-stack. A diagonal Z-plot supports TF-AHR colocalization.

Mechanism of AHR Antagonism in Destabilizing TF

Previously, we demonstrated that IS inhibited TF ubiquitination and degradation.[8] Since AHR activation upregulates TF and AHR antagonists suppress TF, we hypothesized that AHR antagonist enhances TF ubiquitination and degradation. Generally, AHR signaling may regulate TF expression by influencing TF mRNA transcription and/or by modulating TF protein degradation. To distinguish these possibilities, TF expression was examined temporally following treatment with IS and AHR antagonist (Figure 4A). TF levels increased significantly within 2–4 hours of IS treatment; both basal and IS-induced TF were reduced by addition of AHR antagonist (Figure 4A). These changes occurred prior to TF mRNA increase (Supplemental Figure 8), suggesting post-transcriptional regulation.

Since TF protein half-life is controlled by ubiquitination and proteasomal degradation,[8,22] we posited that AHR inhibition enhances TF ubiquitination and degradation. MG132, a potent proteasome antagonist, increased basal and IS-induced TF levels, significantly blocking AHR antagonist-mediated downregulation of both basal and IS-induced TF levels (Figure 4B), suggesting that AHR inhibition increases TF proteasomal degradation. As proteasomal degradation destabilizes protein, we examined TF half-life using emetine, an antagonist of protein translation. AHR inhibition significantly reduced TF half-life in untreated vSMC (from 55 to 22 minutes, Supplemental Figure 9) and IS-treated vSMC (3.25 hours to 40 minutes, Figure 4D). Of note, a significant increase in TF degradation was observed within 30 minutes of AHR antagonist treatment (P=0.04) (Figure 4, C and D).

Ubiquitinated TF undergoes proteasomal degradation in a manner suppressed by IS.[8] That AHR inhibition increased TF degradation through the proteasomal pathway implicates its potential to increase TF ubiquitination. We examined different cell lines, vSMCs and MDA-MB231 (a breast cancer cell line expressing high TF levels).[23] TF ubiquitination was examined using whole cell lysates (Figure 4E) or immunoprecipitated TF (Figure 4F), or with its coexpression with transfected ubiquitin (Figure 4G), all in the presence of MG132. Higher molecular weight– ubiquitinated species of TF accumulated at baseline. The numbers of such species were reduced with IS treatment, suggesting that ligand-bound AHR blocks TF ubiquitination (Figure 4E). CB7993113 increased ubiquitination of TF in a dose-dependent manner in the presence of IS. These data indicate that AHR antagonists enhance TF ubiquitination and proteasomal degradation.

AHR Antagonists as Potential Antithrombotics

As AHR antagonists enhance TF degradation, we evaluated the effectiveness of AHR antagonists as antithrombotics using a validated flow loop model of postinterventional thrombosis.[8,24] This system consists of a silastic tube lined with a monolayer of vSMC, a major trigger for postinterventional thrombosis following endothelial denudation (Figure 5A). The blood flow created by accelerating loops about their vertical axis generates relative wall shear stresses on vSMCs, inducing thrombosis and recapitulating a coronary-like hemodynamic environment experienced in a postinterventional state, as following coronary angioplasty or stenting. Estimates of hemoglobin (Hb; an indicator of the red blood cell component of the clot) and lactate dehydrogenase (LDH; an indicator of the total cellular component of the clot) served as biologic measures of thrombus formation.[8,24] We demonstrated previously that IS robustly induced thrombosis in this model in a TF-dependent manner, as observed in patients with CKD.[8] In the presence of an AHR antagonist, we now show a significant reduction in IS-induced thrombosis (50% reduction in both Hb and LDH, P=0.002 and 0.02, respectively) and uremic serum–induced thrombosis (53%–80% reduction in both Hb and LDH, P=0.02 and $<$0.01, respectively, Figure 5, B–E).

We next examined whether efficacy of AHR antagonism of TF could be correlated with IS levels, which would suggest a putative role as biomarker. AHR antagonist inhibition of vSMCs TF in response to uremic sera from eight ESRD patients (marked with the superscripts "[a]" in Table 1) correlated with

a standard curve generated with a canonical AHR agonist, FICZ (Supplementary Figure 6A). An average of three independent experiments is shown. Compared with control, P values for different IS concentrations were P=0.04 for 0.125, P=0.001 for 0.25, 0.5, and 1.0 μg/ml of IS, and 0.01 for 2.5 and 5.0 μg/ml of IS. Compared with CB7993113, P values for vehicle-treated cells were P=0.01 for 0.025, 0.5, and 1.0 μg/ml of IS, and 0.001 for 2.5 and 5.0 μg/ml of IS. Error bars=SD. The concentrations of free IS at every stage of CKD are shown (Supplemental Figure 4). (E) IS upregulates AHR target genes in vSMCs. vSMCs treated with IS (25 μg/ml) and CH223191 (10 μM) for 24 hours. Samples treated with HSA served as controls. Quantitative RT-PCR reactions were run in duplicate for each sample and quantified using real-time PCR for detecting *Cyp1b1*, *Cyp1a1*, and *Ahrr* mRNA and the ct (cycle threshold) values were generated. An average of three independent experiments performed in duplicates is shown. Error bars=SEM. Compared with control, the IS had higher *Cyp1b1*, $P<0.01$, *Cyp1a1*, P=0.001, and *Ahrr*, P=0.01. Compared with control, CH223191-treated samples had lower *Cyp1b1 and Cyp1a1*, P=0.02 and *Ahrr*, P=0.005. Compared with IS, the IS+CH223191 had lower AHR target genes. *Cyp1b1*, P=0.01, *Cyp1a1*, P=0.001, and *Ahrr*, P=0.002. (F) AHR antagonist abrogates downregulation of AHR induced with uremic serum. vSMCs treated with calf serum (CS) or control and uremic serum for 12 hours were harvested. The values below the blot represent the normalized bands against the loading control using ImageJ. A representative of three independent experiments is shown.

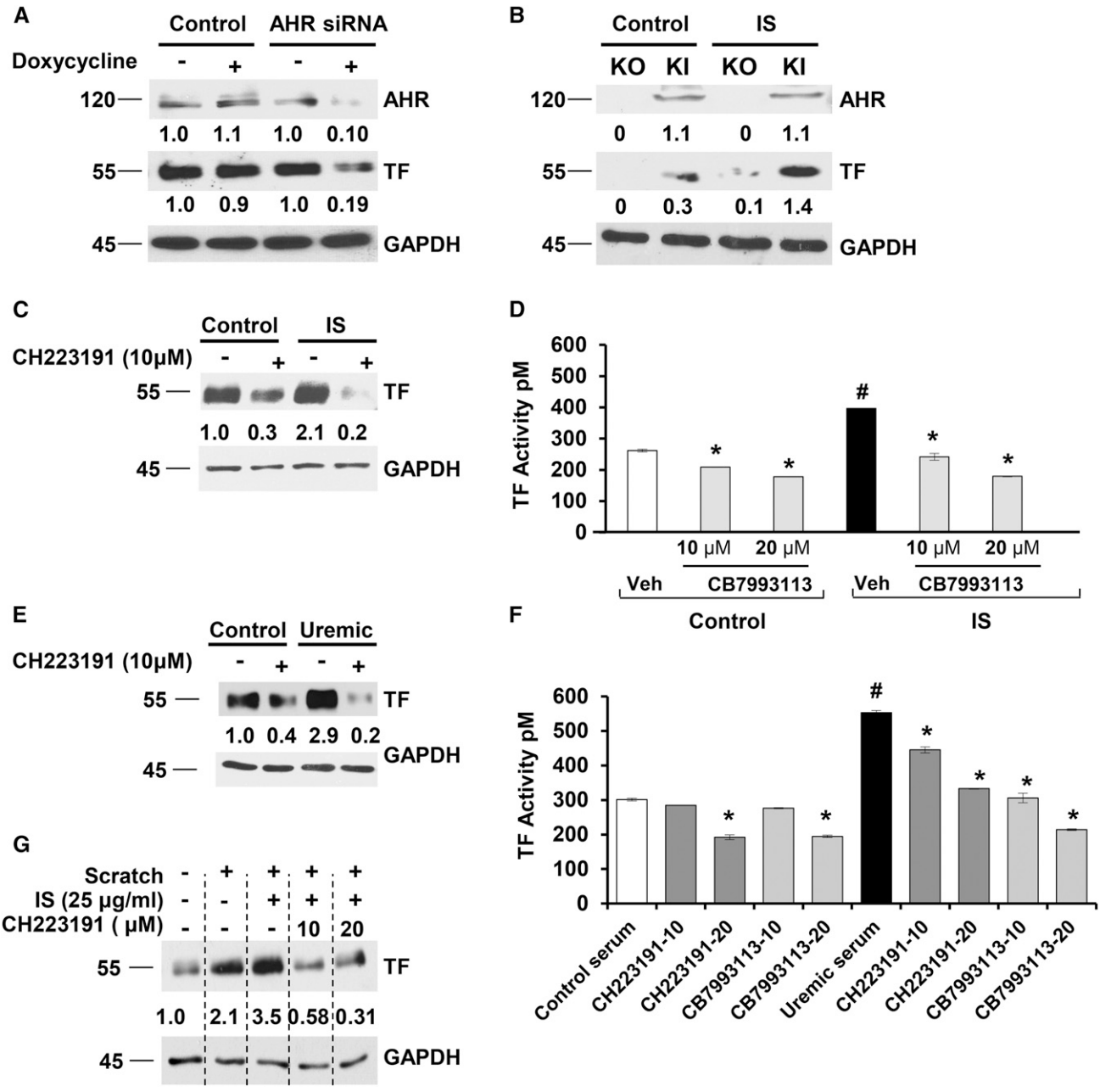

Figure 2. Uremic serum and IS regulate both basal and IS-mediated TF levels through AHR signaling. (A) *AHR* silencing reduces basal TF expression. vSMCs stably expressing control or doxycycline-inducible AHR short hairpin RNA were treated with doxycycline for 48 hours. The values below the blot represent the bands normalized to the loading control using ImageJ. A representative of four independent experiments is shown. P=0.001 for TF levels between doxycycline-induced control and AHR short hairpin RNA. (B) $AHR^{-/-}$ knockout (KO) MEFs exhibit reduced TF compared with AHR KI MEFs. MEFs from KO and KI mice were withdrawn from doxycycline for 5 days and treated with 25 μg/ml IS for 24 hours. A representative of three independent experiments is shown. P=0.001 for TF between IS-treated KO and KI cells. (C) AHR antagonist downregulates IS-induced TF expression. vSMCs treated with 25 μg/ml IS and CH223191 for 24 hours. A representative of five independent experiments is shown. P=0.02 for control with and without AHR antagonist; and P=0.001 for IS with and without AHR antagonist. (D) AHR antagonist suppresses IS-induced procoagulant TF activity. vSMCs treated with 25 μg/ml IS and CB7993113 (10 μM) for 24 hours and subjected to procoagulant TF activity on intact vSMCs. An average of three independent experiments performed in duplicates is shown. Error bars =SD. The P values were as follows: $P<0.01$ between control and IS; P=0.02 between control and control+10 μM and P=0.008 for 20 μM CH223191; P=0.03 between IS and IS+10 μM and P=0.003 for 20 μM CH223191. (E) AHR antagonist downregulates both the control and uremic serum–induced TF expression. vSMCs treated with 5% pooled control or uremic serum and CB7993113 for 24 hours. A representative of five independent experiments is shown. Compared with control serum–treated cells P=0.02 for control serum with AHR antagonist; compared with uremic serum P=0.001 for uremic

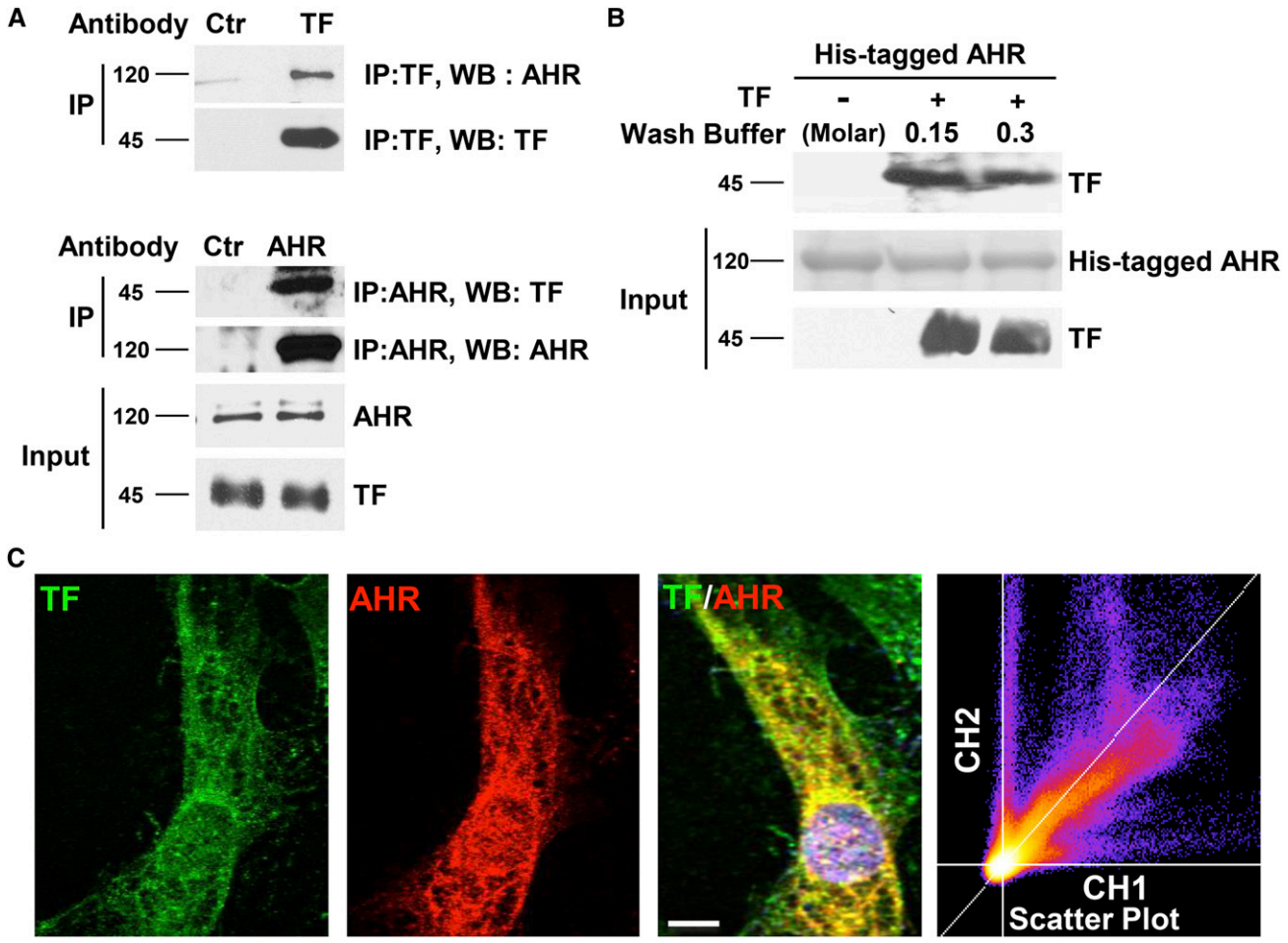

Figure 3. AHR directly binds to TF. (A) TF and AHR reciprocally coimmunoprecipitate. Lysates of vSMCs were immunoprecipitated using TF or AHR or respective isotype control antibodies. Five percent of the cell lysates was probed for TF and AHR as input. A representative from four independent experiments is shown. (B) Purified recombinant His-tagged human AHR (hAHR) interacts with purified recombinant human TF. His-tagged hAHR on nickel resin were treated with recombinant TF for 4 hours at 4°C and washed with buffer containing sodium chloride at different concentrations as shown and resolved on SDS-PAGE gel. Five percent of recombinant His-tagged AHR (Ponseau stain) and recombinant TF (immunoblot) are shown as inputs. A representative immunoblot from two experiments is shown. (C) TF and AHR colocalize. vSMCs were stained for TF and AHR and imaged using confocal microscopy. Representative images from 100 randomly counted cells are shown. Scatter plots were generated with TF on channel 1 and AHR on channel 2 using ImageJ. The plots pointing along the *X* or *Y* axes represent the absence of colocalization, whereas that pointing along the *Z* axis indicates colocalization. The Pearson correlation coefficient for AHR and TF was 0.84 as calculated by ImageJ. Scale bar, 10 μM.

serum IS levels (Spearman correlation coefficient=0.85, $P<0.01$, Figure 5F). As free IS is biologically active and expected to represent 10% of total IS (Supplemental Table 4), it is likely that 10 μM of AHR antagonist sufficiently antagonized estimated free IS (average$\pm$SD of 5.11$\pm$2.33 μg/ml). Correlation of IS levels with the AHR antagonist effect on TF supports further development of IS as a putative efficacy biomarker.

serum with AHR antagonist. (F) AHR antagonists suppress procoagulant TF activity in both control and uremic sera–treated vSMCs. vSMCs were treated with 5% pooled control or uremic serum and AHR antagonist for 24 hours and TF activity was measured. An average of three independent experiments is shown. Error bars=SD. The *P* values were as follows: $P=0.003$ between control and uremic serum; for the control group, $P=0.14$ between control serum and control serum+10 μM CH223191 and $P=0.02$ with 20 μM CH223191, and $P=0.08$ for control serum+10 μM and $P=0.007$ for 20 μM CB7993113; for the uremic group, $P=0.04$ between uremic serum and uremic serum+10 μM and $P<0.01$ for 20 μM CH223191, and $P=0.02$ for uremic serum+10 μM and $P=0.002$ for 20 μM CB7993113. (G) AHR antagonist suppresses combined injury and IS-augmented TF upregulation. vSMCs treated with IS and CH223191 for 24 hours were injured using a cell scrapper. The cells were harvested after 2 hours. A representative from three experiments is shown. $P=0.05$ for TF between combined IS+injury without and with AHR antagonist.

DISCUSSION

We demonstrate that AHR signaling plays a critical role in regulating vSMC TF levels. This regulation is of particular relevance to patients with renal failure and uremia following vascular injury. IS, a uremic toxin, activates AHR, which then interacts directly with and stabilizes TF, promoting thrombosis. Conversely, suppression of AHR activity by AHR antagonists ubiquitinates and destabilizes TF, an effect that we found robustly inhibited thrombosis despite exposure to IS or a uremic milleu. We reveal AHR's potential as a novel antithrombotic target in patients with renal failure, a fact strengthened by correlations between IS levels and AHR/TF activities in humans, as well as IS correlation with AHR antagonist responsiveness. Our work focuses on vSMCs as the major trigger of postinterventional thrombosis, yet the IS-AHR-TF axis may well extend to other types of thrombosis, such as AVF thrombosis or spontaneous venous thrombosis, whose incidence also remain higher in CKD patients.[1,25]

Traditionally, AHR is recognized as a receptor for exogenous and endogenous toxins. That AHR activation upregulates several detoxifying enzymes such as *Cyp1a1* and *Cyp1b1*, *etc.*,[26] supports its function as a sensor and detoxifier of environmental chemicals. Therefore AHR may similarly serve as a receptor for IS, an endogenous toxin. AHR is a transcriptional regulator[26] and also assists protein degradation.[14,15] The present data in vSMCs pertinent to the thrombosis model point to a divergent role of AHR from its currently accepted pathophysiologic role as a transcriptional coactivator.

AHR can potentially regulate TF at multiple levels: gene, mRNA, and protein. A role in transcriptional regulation has recently been described by Gondouin *et al.*[20] In ECs and polymorphonuclear cells, IS upregulated TF transcription through AHR signaling.[20] IS increased TF mRNA at the end of 4 hours and TF protein expression by 6 hours.[20] In contrast, we demonstrate that AHR rapidly regulates vSMC TF at the protein level as substantiated by the following observations: (*1*) AHR antagonists shorten TF half-life, resulting in its degradation within 30 minutes indicating a post-transcriptional mechanism (Figure 4, C and D); (*2*) AHR antagonist-mediated TF downregulation is abrogated with proteasomal blocking (Figure 4B); and (*3*) AHR antagonists enhance TF ubiquitination (Figure 4, C–G). Althought not specifically studied, such post-translational regulation of TF may also be present in ECs.[20] Our data indicate a direct interaction (Figure 3B) and regulation of TF through AHR; however, an indirect regulation is also likely.[27] All of these data support multiple mechanisms of AHR-mediated TF regulation in different cell types underscoring its critical role in TF biology.

ECs and vSMCs exhibit distinct roles in thrombosis. Venous thromboembolic diseases is characterized by clot formation often precipitated by flow stasis on dysfunctional, albeit generally intact, endothelium.[20] In contrast, vSMCs, are the major cell type exposed to blood following arterial injury.[6] Cardiovascular and cerebrovascular thrombotic events are precipitated by clot formation at sites of endothelial disruption following plaque rupture or interventions such as angioplasty or stenting, wherein endothelium is directly removed, making vSMC the relevant contributor. Indeed, re-endothelialization to cover thrombogenic vSMCs is the hallmark of vascular healing and heralds the reduction in postinterventional clotting risk. Despite vastly different functions of endothelium and vSMCs, the current work, and that of others[20] suggests that IS-mediated TF regulation through AHR enhances both venous and arterial thrombosis in CKD.

Most contemporary antithrombotics target factors of coagulation in blood, rather than targeting the vascular wall compartment, as with the AHR antagonism. Recently, geldanamycin was examined as an indirect AHR suppressor and found to reduce TF,[20] yet it has many limitations. As a HSP90 antagonist, it inhibits key chaperon activities causing degradation of a number of vital proteins, including kinases such as mitogen-activated protein kinase.[20] Indeed, geldanamycin's effect on TF mRNA may not entirely be through AHR-dependent pathways as it suppresses the mitogen-activated protein kinase pathway,[28] itself a potent inducer of TF mRNA in ECs.[9] Lack of overall specificity resulting in many off-target effects makes geldanamycin a therapeutically undesirable option.[29]

In contrast, targeted AHR antagonism with novel inhibitors such as CB7993113 is a promising antithrombotic approach in CKD-mediated thrombosis. Historically, managing thrombosis in CKD patients has proven challenging. Pharmacokinetics limits agent selection[30] whereas retained products augment bleeding risk.[31] Conventional antithrombotics have consistently proven inadequate in CKD in numerous clinical scenarios.[6,32,33] As renal deterioration progresses, vascular cells are exposed to increasing levels of IS, perpetuating the prothrombotic milieu. Even at concentrations found in early CKD patients, IS induces TF activity in vSMCs (Supplemental Figure 10). While the standard approach to managing uremic toxins is removal through dialysis, IS is highly protein bound and is poorly cleared.

AHR antagonism provides a novel way of managing uremic toxins, not through clearance, but through abrogating toxic effects through their intracellular mediator–AHR pathway. Employing a flow loop model of postinterventional thrombosis relevant to CKD,[8,24,34] we demonstrate potent inhibition of IS-induced or uremic serum–induced thrombosis in vSMCs (Figure 5). Correlations between components of the IS-AHR-TF axis in CKD patients support the relevance of AHR as a potential target in humans (Table 2). Targeting AHR directly with AHR antagonists is expected to have fewer off-target effects and may even offer unique advantages with respect to bleeding. While most antithrombotics target blood-borne coagulation components systemically, thus increasing bleeding risks in uremic patients,[30,31] AHR antagonists may preferentially act at sites of local vascular damage (*i.e.*, the vSMC compartment), despite systemic administration.

Linking diagnostic biomarkers with targeted AHR antagonists is a further way to improve the antithrombotic risk-benefit

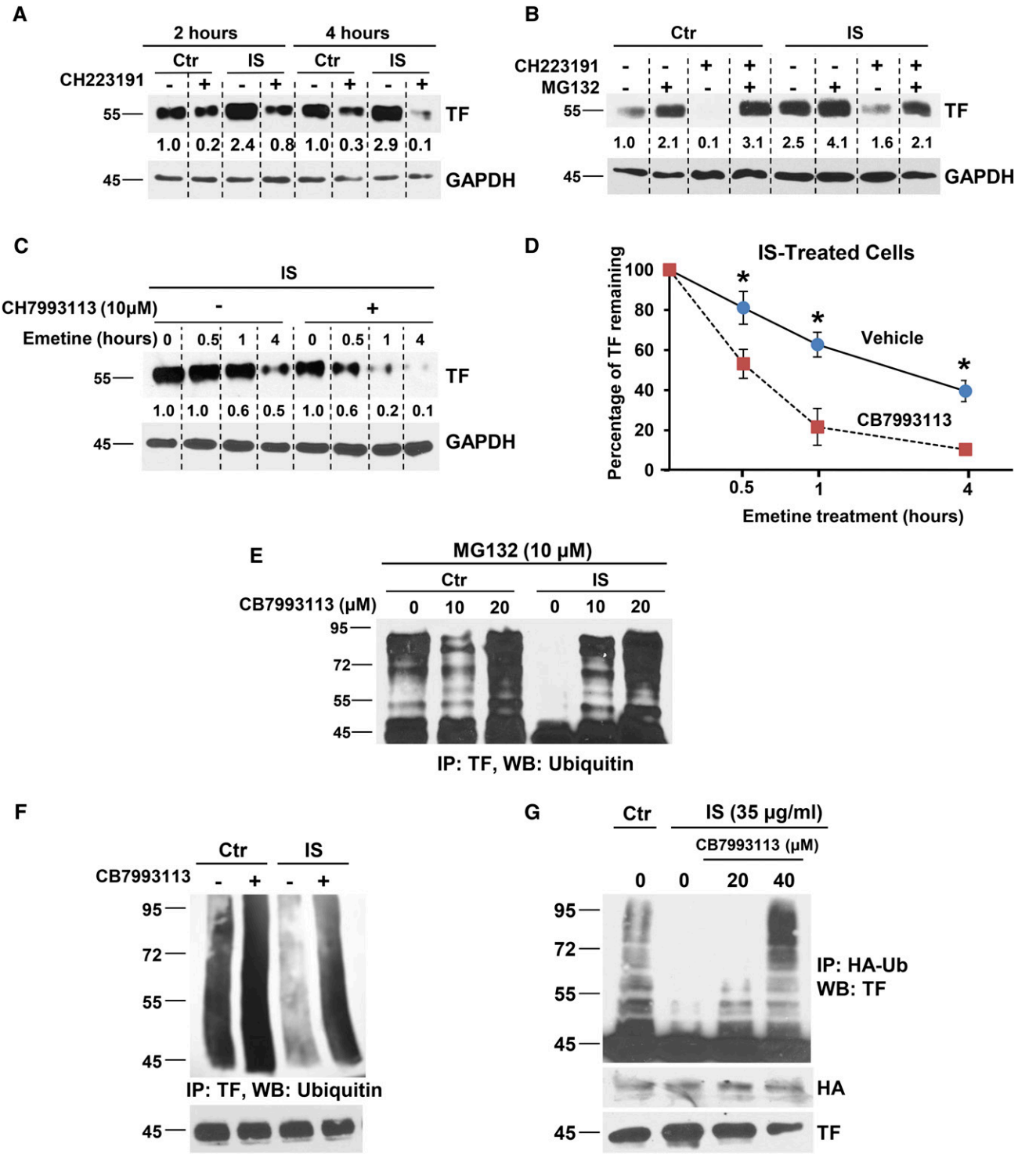

Figure 4. TF regulation by IS and AHR antagonists. (A) IS induces and AHR antagonist suppresses TF within 2 hours of treatment. vSMCs treated with 25 μg/ml IS and 10 μM CH223191 for the indicated time. A representative of three independent experiments is shown. (B) Proteasome inhibition abrogates the effect of an AHR antagonist on both basal and IS-induced TF levels. vSMCs treated for 4 hours with 10 μM proteasome inhibitor (MG132) and 2 hours with 25 μg/ml IS and 10 μM AHR antagonist (CH223191) were lysed and probed. A representative of three independent experiments is shown. (C) AHR antagonist destabilizes IS-induced TF. vSMCs treated with 25 μg/ml IS and CB7993113 for 24 hours were treated with 20 μM emetine and harvested at the indicated time. A representative from three experiments is shown. (D) Densitometry was performed using ImageJ. GAPDH was used to normalize the TF signal. An average of three independent experiments is shown. Error bars=SD. *P*=0.01 for TF levels compared with and without CB7993113 for

through patient selection. Indeed, we found that IS levels varied dramatically in individuals with CKD, even among those in the same CKD stage (stage V=7–8-fold; Table 1). Moreover, this IS level exhibited a dose-response relationship with TF expression and activity across the entire spectrum of CKD (Supplemental Figure 10). Thus, IS measurement may well be a suitable biomarker to stratify thrombosis risk in CKD patients. Moreover, as IS levels correlated with responsiveness to AHR antagonists in the vSMC compartment (Figure 5E), it may be further leveraged to select patients and refine AHR antagonist management.

Of note, AHR antagonists downregulated TF in cells exposed to control serum (nonuremic), albeit to a lesser extent (Figure 2, E and F). Several endogenous ligands can constitutively activate AHR signaling[35,36] and may regulate a "tonic" level of TF on which AHR antagonists can act. Thus, AHR antagonists may represent an important approach to limiting thrombosis even in a nonuremic cohort.

To allow integrated studies between vSMCs, uremic toxins, and reactive whole blood, we employed a flow loop model and demonstrated the potential of AHR antagonists as a novel class of antithrombotics (Figure 5). While experiments in an animal model would have been desirable, murine models of CKD fail to recapitulate the enhanced thrombotic phenotype following vascular injury[37] that was critical to our work. Therefore, we opted for a "humanized" system with human serum to generate a response in human vSMCs exposed to human blood perfused at human coronary flow conditions. Importantly, we have already demonstrated that this model recapitulates the increased thrombosis of the CKD milieu.[8]

In addition to the lack of an animal model, this study has limitations. First, the concentrations of IS and HSA used to treat cells corresponded to the levels found in ESRD patients[25,38–41] and this combination of HSA and IS is expected to result in 10% of the free form of IS, a biologically active form. Although lack of direct measurement of free IS represents a limitation of the study, the conditions used were sufficient to activate AHR signaling and TF stabilization. Second, 20 patients is a small sample size; however, the demonstration of statistically significant results even in such a small group, supports potential future studies in larger cohorts. Third, the above experiments examined the effects of IS or AHR signaling from 20 minutes to 48 hours. As we begin to explore AHR-mediated effects in this relatively short time frame, it will be critical to also determine the effect of chronic IS exposure of vSMCs.

IS is a member of an emerging group of prothrombotic metabolites termed as "thrombolome"[25]. Overall, this work delineates a mechanism of the prothrombotic property of IS and, in doing so, defines AHR as an antithrombotic target and AHR antagonists as a novel class of antithrombotics. The combination of IS levels and AHR antagonists forms the foundation for a unique theranostic antithrombotic platform in CKD patients.

CONCISE METHODS

Please refer to the Data Supplement for expanded methods for human samples (human subjects and serum collection, immunohistochemistry for AHR and TF), biochemical experiments (cell lines, reagents, lysis and immunoblotting, immunoprecipitation, immunofluorescence, and chemical synthesis of direct AHR antagonist CB7993113, bacloviral protein production, and *in vitro* interaction), and cell biologic experiments (*in vivo* ubiquitination assay, procoagulant TF activity assay, and AHR activity assay).

Liquid Chromatography/Mass Spectrometry Method for Determination of IS

Briefly, 20 μl of serum samples, or IS standards were diluted with 40 μl of water. Fifty microliters of the diluted sample was mixed with 200 μl of acetonitrile containing internal standard (deuterated IS). The mixture was filtered with a 96-well protein crash plate. Forty microliters of filtrate was mixed with 160 μl of 5 mmol/l ammonium acetate. The injection volume was 50 μl. An Agilent 1200 pump was used for separation. Samples were loaded onto a C18 analytical column and eluted with a binary gradient consisting of solvent A (5 mmol/l ammonium acetate solution) and solvent B (methanol). Mass spectrometry was performed using a API 400 triple quadrupole mass spectrometry with the electrospray source in negative mode. Tandem mass spectrometer parameters were set as follows: DP −48.0, EP −10, GS1 4.0, NC −1.0, CAD 6.0, and TEM 300°C. MRM was used for the multiple products of IS (212>80.0) and IS-d4 (216>80) (Supplemental Figure 1A).

Cell Lines and Treatment of Uremic Toxins

Primary human aortic vSMCs obtained from the American Type Culture Collection (ATCC) were grown in DMEM low glucose with 5% calf serum and 1% penicillin and streptomycin and used for up to 10 passages. Rat vSMCs (A57r), MDA-MB231, and HepG2 cells (all obtained from ATCC) were grown in DMEM high glucose with 10% FBS and 1% penicillin and streptomycin. Early passage AHR KO-KI

a given time point. (E) Suppression of AHR activity enhances TF ubiquitination. vSMCs treated with control or 25 μg/ml IS with or without CB7993113 for 24 hours and MG132 for 4 hours were lysed and probed using TF antibody. A representative of two independent experiments is shown. (F) AHR antagonist increases ubiquitination of basal TF and also restores IS-inhibited TF ubiquitination. vSMCs were treated as above and immunoprecipitated using TF antibody and immunoblotted with ubiquitin antibodies. Immunoprecipitated TF is shown as input. A representative from three experiments is shown. (G) AHR antagonist increases TF ubiquitination. MDA-MB231 cells were transfected with HA-ubiquitin and then treated with 25 μg/ml IS and CB7993113 for 24 hours and 10 μM MG132 for 16 hours. Cells lysed in RIPA buffer were immunoprecipitated using HA antibody and immunoblotted with TF antibody. Five percent of the cell lysates was probed for TF and HA as inputs. A representative immunoblot from three experiments is shown. GAPDH, glyceraldehyde-3-phosphoate dehydrogenase.

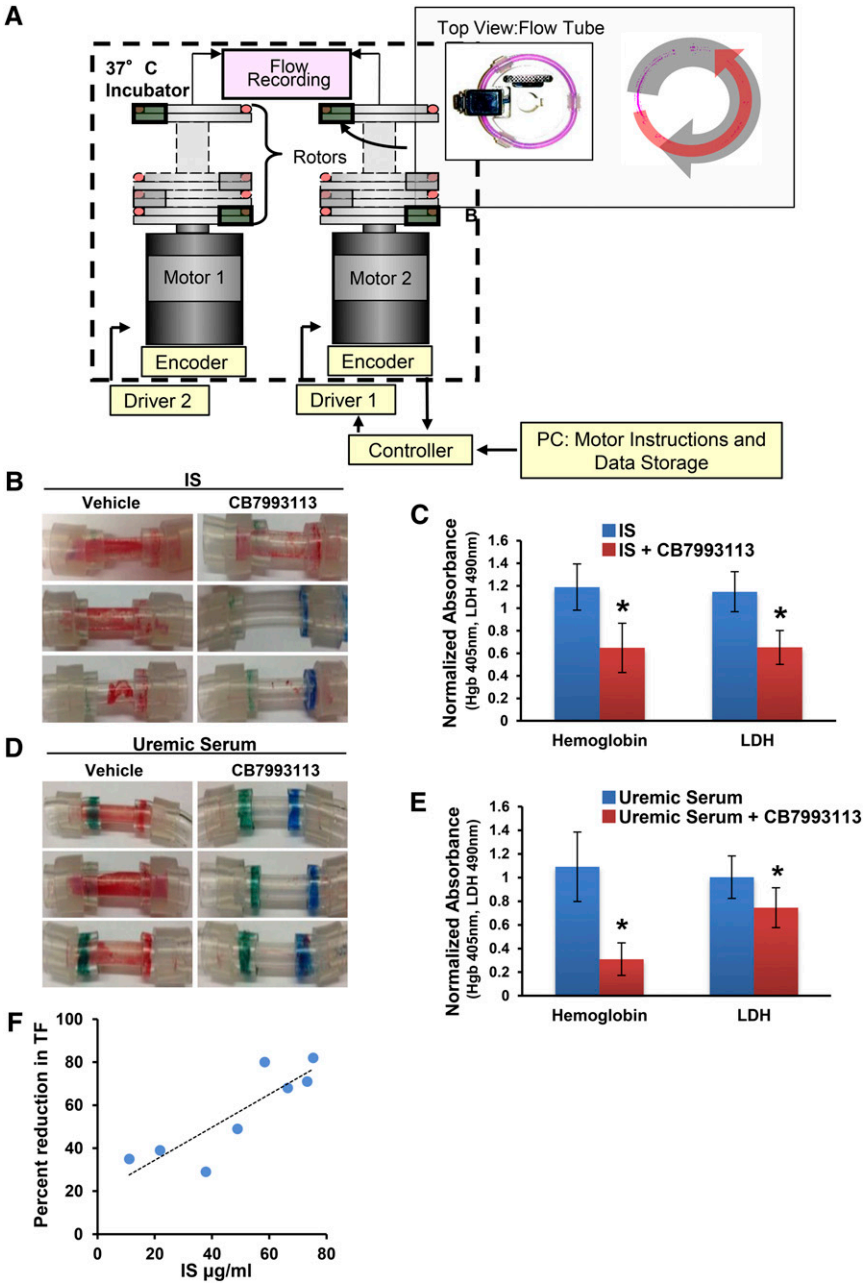

Figure 5. A novel AHR antagonist suppresses thrombosis in a postendovascular interventional thrombosis model. (A) Flow loop model design. The flow loop system consists of silastic loops with a reactive segment lined by vSMCs loaded on rotor stages driven by motors and motion controllers. The entire rotor system is held within an incubator at 37°C and driven by motors connected remotely to the controllers, circuitry, and flow recorders. The wall motion creates bidirectional flows that are measured via onboard, extracorporeal flow probes built into the rotor stages. (Insert) Arial view of a loop, which fits onto the rotor stage and is placed in axial alignment. (B) Thrombogenicity of IS is significantly abrogated by AHR antagonist CB7993113. vSMCs grown on fibronectin-coated tubes were exposed to 25 μg/ml IS with or without 20 μM CB7993113 for 24 hours. The tubes were then loaded with blood in the flow loop system. Three representative flow loop tubes showing inhibition of clot formation are shown. (C) Hb and LDH values of the thrombi from flow loop tubes treated with IS with or without AHR antagonist are shown. An average of six independent tubes is shown. P=0.002 for Hb and P=0.02 for LDH of uremic serum compared with the control serum. Error bars=SEM. (D) An AHR antagonist significantly abrogates thrombogenicity of uremic sera. vSMCs grown on fibronectin-coated tubes were exposed to pooled 5% uremic serum with or without 20 μM CB7993113 for 24 hours. The tubes were then subjected to shear forces in the flow loop system with blood flowing on the surface. Three representative flow loop tubes for visual examination of the clot are shown. (E) Hb and LDH values of the thrombi from the flow loop tubes treated with uremic serum with or without an AHR antagonist are shown. The data are averaged from six tubes. P=0.02 for Hb and P<0.01 for LDH of uremic serum compared with the control serum. Error bars=SEM. (F) AHR antagonist efficacy in reducing TF correlates with IS levels. vSMCs were treated with sera from eight individual ESRD patients (marked with superscript "a" in Table 1) with 10 μM of CH223191. Percent reduction in TF expression in CH223191-treated cells was compared with vehicle-treated cells. Average TF reduction from two independent experiments was correlated with IS levels.

MEFs (a gift from Dr. A. Puga, University of Cincinnati)[21] were grown in F12 medium supplemented with 10% FBS (Life Technologies), 26 mM $NaHCO_3$, 1% antibiotic/antimycotic solution (Sigma-Aldrich), and 600 ug/ml G418 (GIBCO Invitrogen Corporation) to ensure retention of the $AHR^{-/-}$ genotype generated by insertion of the bacterial neo gene. Stable transfectant clones expressing AHR protein (KI) were grown in the same medium containing an additional 3 μg/ml puromycin (A.G. Scientific, Inc.) and 400 μg/ml hygromycin (Calbiochem). Doxycycline (Sigma-Aldrich), a tetracycline analog, was used at a final concentration of 5 μg/ml to suppress the expression of AHR. Doxycycline was withdrawn for 5 days to allow expression of AHR. Wild-type C57BL/6 background MEFs were grown in F12 medium supplemented with 10% FBS and antibiotics.

The cells were treated with the HSA and IS corresponding to the average concentrations found in the serum of ESRD patients of albumin and IS (total) of 4.0 gm/dl and 25 μg/ml, respectively, which is known to result in 1–2.5 μg/ml of the free form of IS (4%–10% of total).[38–40] HSA was purchased from Lee Biosolutions (St. Louis, MO) and for the bound form, IS was incubated for 15 minutes at room temperature in medium containing FBS supplemented with HSA to bring up to a final concentration of albumin of 4.0 gm/dL. Unless specified, all the figures

in this article utilized the bound form of IS and thus HSA served as a control. No free form of IS was measured in the medium under these conditions. For the experiments with the free form of IS, cells were treated with IS in serum- and albumin-free medium (Figure 1D).

Flow Loop System

A flow loop consists of silastic tubes coated with human vSMCs subjected to coronary flow conditions that emulate the endovascular intervention *ex vivo* and serve as a screening tool to examine thrombosis in various vascular beds. Prior to cell seeding, 4-cm-long, 1/8" ID Tygon® tubes (Saint-Gobain, France) were prepared as described previously[8,24,34] and injected with 1×10^6 cells/ml vSMCs into the fibronectin-coated tubes and cultured for 16 hours under axial rotation at 10 rph, 37°C, 5% CO_2.

vSMC coated tubes were exposed to uremic serum (5%) or IS (5 μg/ml, without HAS) with or without 40 μM CB7993113 for 24 hours. The segments were explanted, gently flushed to remove the media, and positioned in the reactive site flow loop model as described (Figure 5A).[8,24,34] Fresh whole blood was collected from healthy volunteers in a 10% acid-citrate dextrose solution. Immediately prior to testing, a 100 mM/l $CaCl_2$/75 mM/l $MgCl_2$ solution was added to the blood (70 μl solution per 1 ml blood) and loaded into the flow loops. After 10-minute runs, the loops were emptied and flushed with 60 ml Tyrodes buffer (0.01 mol/L HEPES, 0.75 mM/l $MgCl_2$) to remove nonadherent material. The clot was lyzed with 1% Triton-X solution for 20 minutes. LDH and Hb were measured using Quantichorme Heme Assay and Cyto-Tox 96 Non-Radioactive Cytotoxicity Assay (Promega) as measures of total clot and erythrocyte content, respectively.

Statistical Analyses

Summary statistics are presented as the mean, median, and SD. Either a paired-*t* test or a Wilcoxon rank sum test was performed to compare the groups as appropriate. Spearman or Pearson correlation was performed to analyze the correlation between two variables, as appropriate. Statistical significance was assessed at the $P<0.05$ level. A one-way ANOVA with Dunnett's *post hoc* test was used to compare the half maximal effective concentration with CB7993113.

ACKNOWLEDGMENTS

The authors acknowledge Dr. David Salant (Boston University School of Medicine [BUSM]) for helpful discussions throughout the development of this work and for reviewing the manuscript, and thank both Dr. Nigel Mackman (University of North Carolina) for the development of the procoagulant TF activity assay and Dr. A. Puga (University of Cincinnati) for providing AHR KO and KI cells. We acknowledge Drs. Grace Zhao, Tan Josenia, and Elena Metrikova for immunohistochemistry, Olga Novikov for RT-PCR (all at BUSM), and Fernando Polite (Universitat Ramon Llull, and Massachusetts Institute of Technology) for their technical assistance. We thank Drs. William Chan (Pacific University) for bacloviral particles for AHR and Irene Bosch (Massachusetts Institute of Technology) and Nader Rahimi (BUSM) for bacloviral AHR protein production. We appreciate Jamaica Siwak (BUSM) for proofreading the manuscript.

This work was funded in part by grant NIH/NIDDK K08-DK080946 (V.C.C.), grant P42-ES007381 and the Art BeCAUSE Breast Cancer Foundation (D.H.S.), a Sharon Anderson Research Fellowship grant award from the American Society of Nephrology (M.S.), an AHA Fellow to Faculty Transition grant 12FTF12080241 (K.K.), grant RO1GM-49039 (E.R.E.), and by grant BFU2009-09804 from Spain's Ministerio de Ciencia e Innovación, by Posimat, and by Fundació Empreses IQS (M.B.).

A part of this work was submitted as an abstract at the 2015 Annual American Society of Nephrology meeting on November 4–8, San Diego, CA.

V.C.C. and D.H.S designed the research, S.S., M.S., and L.A. performed the experiments, Mo.B. performed the immunofluorescence studies, K.K, Me.B., and E.R.E. designed and performed the flow loop experiments, and M.S. and J.F. collected and compiled the human data. A.Z. performed the metabolomics screen, J.W. guided the statistical analysis, S.S, M.S., Mo.B., and V.C.C prepared the figures, V.C.C, prepared the manuscript, and D.H.S., E.R.E, and K.K. edited the manuscript.

DISCLOSURE

None.

REFERENCES

1. Casserly LF, Dember LM: Thrombosis in end-stage renal disease. *Semin Dial* 16: 245–256, 2003
2. Kumar G, Sakhuja A, Taneja A, Majumdar T, Patel J, Whittle J, Nanchal R; Milwaukee Initiative in Critical Care Outcomes Research (MICCOR) Group of Investigators: Pulmonary embolism in patients with CKD and ESRD. *Clin J Am Soc Nephrol* 7: 1584–1590, 2012
3. Kimura T, Morimoto T, Kozuma K, Honda Y, Kume T, Aizawa T, Mitsudo K, Miyazaki S, Yamaguchi T, Hiyoshi E, Nishimura E, Isshiki T; RESTART Investigators: Comparisons of baseline demographics, clinical presentation, and long-term outcome among patients with early, late, and very late stent thrombosis of sirolimus-eluting stents: Observations from the Registry of Stent Thrombosis for Review and Reevaluation (RESTART). *Circulation* 122: 52–61, 2010
4. Iakovou I, Schmidt T, Bonizzoni E, Ge L, Sangiorgi GM, Stankovic G, Airoldi F, Chieffo A, Montorfano M, Carlino M, Michev I, Corvaja N, Briguori C, Gerckens U, Grube E, Colombo A: Incidence, predictors, and outcome of thrombosis after successful implantation of drug-eluting stents. *JAMA* 293: 2126–2130, 2005
5. Belardi JA, Albertal M: Coronary stent thrombosis in patients with chronic kidney disease: balancing anti-ischemic efficacy and hemorrhagic risk. *Catheter Cardiovasc Interv* 80: 368–369, 2012
6. Park SH, Kim W, Park CS, Kang WY, Hwang SH, Kim W: A comparison of clopidogrel responsiveness in patients with versus without chronic renal failure. *Am J Cardiol* 104: 1292–1295, 2009
7. James S, Budaj A, Aylward P, Buck KK, Cannon CP, Cornel JH, Harrington RA, Horrow J, Katus H, Keltai M, Lewis BS, Parikh K, Storey RF, Szummer K, Wojdyla D, Wallentin L: Ticagrelor versus clopidogrel in acute coronary syndromes in relation to renal function: results from the Platelet Inhibition and Patient Outcomes (PLATO) trial. *Circulation* 122: 1056–1067, 2010
8. Chitalia VC, Shivanna S, Martorell J, Balcells M, Bosch I, Kolandaivelu K, Edelman ER: Uremic serum and solutes increase post-vascular interventional thrombotic risk through altered stability of smooth muscle cell tissue factor. *Circulation* 127: 365–376, 2013

9. Steffel J, Lüscher TF, Tanner FC: Tissue factor in cardiovascular diseases: molecular mechanisms and clinical implications. *Circulation* 113: 722–731, 2006
10. Vanholder R, Baurmeister U, Brunet P, Cohen G, Glorieux G, Jankowski J; European Uremic Toxin Work Group: A bench to bedside view of uremic toxins. *J Am Soc Nephrol* 19: 863–870, 2008
11. Jourde-Chiche N, Dou L, Cerini C, Dignat-George F, Vanholder R, Brunet P: Protein-bound toxins—update 2009. *Semin Dial* 22: 334–339, 2009
12. Stejskalova L, Dvorak Z, Pavek P: Endogenous and exogenous ligands of aryl hydrocarbon receptor: current state of art. *Curr Drug Metab* 12: 198–212, 2011
13. Puga A, Ma C, Marlowe JL: The aryl hydrocarbon receptor cross-talks with multiple signal transduction pathways. *Biochem Pharmacol* 77: 713–722, 2009
14. Kawajiri K, Kobayashi Y, Ohtake F, Ikuta T, Matsushima Y, Mimura J, Pettersson S, Pollenz RS, Sakaki T, Hirokawa T, Akiyama T, Kurosumi M, Poellinger L, Kato S, Fujii-Kuriyama Y: Aryl hydrocarbon receptor suppresses intestinal carcinogenesis in ApcMin/+ mice with natural ligands. *Proc Natl Acad Sci U S A* 106: 13481–13486, 2009
15. Ohtake F, Baba A, Takada I, Okada M, Iwasaki K, Miki H, Takahashi S, Kouzmenko A, Nohara K, Chiba T, Fujii-Kuriyama Y, Kato S: Dioxin receptor is a ligand-dependent E3 ubiquitin ligase. *Nature* 446: 562–566, 2007
16. Schroeder JC, Dinatale BC, Murray IA, Flaveny CA, Liu Q, Laurenzana EM, Lin JM, Strom SC, Omiecinski CJ, Amin S, Perdew GH: The uremic toxin 3-indoxyl sulfate is a potent endogenous agonist for the human aryl hydrocarbon receptor. *Biochemistry* 49: 393–400, 2010
17. Bogdanov VY, Osterud B: Cardiovascular complications of diabetes mellitus: The Tissue Factor perspective. *Thromb Res* 125: 112–118, 2010
18. Parks AJ, Pollastri MP, Hahn ME, Stanford EA, Novikov O, Franks DG, Haigh SE, Narasimhan S, Ashton TD, Hopper TG, Kozakov D, Beglov D, Vajda S, Schlezinger JJ, Sherr DH: In silico identification of an aryl hydrocarbon receptor antagonist with biological activity in vitro and in vivo. *Mol Pharmacol* 86: 593–608, 2014
19. Zhao B, Degroot DE, Hayashi A, He G, Denison MS: CH223191 is a ligand-selective antagonist of the Ah (Dioxin) receptor. *Toxicol Sci* 117: 393–403, 2010
20. Gondouin B, Cerini C, Dou L, Sallée M, Duval-Sabatier A, Pletinck A, Calaf R, Lacroix R, Jourde-Chiche N, Poitevin S, Arnaud L, Vanholder R, Brunet P, Dignat-George F, Burtey S: Indolic uremic solutes increase tissue factor production in endothelial cells by the aryl hydrocarbon receptor pathway. *Kidney Int* 84: 733–744, 2013
21. Chang X, Fan Y, Karyala S, Schwemberger S, Tomlinson CR, Sartor MA, Puga A: Ligand-independent regulation of transforming growth factor beta1 expression and cell cycle progression by the aryl hydrocarbon receptor. *Mol Cell Biol* 27: 6127–6139, 2007
22. Mackman N: Uremic serum and ubiquitylation of tissue factor. *Circulation* 127: 320–321, 2013
23. Pendurthi UR, Ghosh S, Mandal SK, Rao LV: Tissue factor activation: is disulfide bond switching a regulatory mechanism? *Blood* 110: 3900–3908, 2007
24. Kolandaivelu K, Swaminathan R, Gibson WJ, Kolachalama VB, Nguyen-Ehrenreich KL, Giddings VL, Coleman L, Wong GK, Edelman ER: Stent thrombogenicity early in high-risk interventional settings is driven by stent design and deployment and protected by polymer-drug coatings. *Circulation* 123: 1400–1409, 2011
25. Shashar M, Francis J, Chitalia V: Thrombosis in the uremic milieu-emerging role of "thrombolome". *Semin Dial* 28: 198–205, 2015
26. Barouki R, Aggerbeck M, Aggerbeck L, Coumoul X: The aryl hydrocarbon receptor system. *Drug Metabol Drug Interact* 27: 3–8, 2012
27. Yisireyili M, Saito S, Abudureyimu S, Adelibieke Y, Ng HY, Nishijima F, Takeshita K, Murohara T, Niwa T: Indoxyl sulfate-induced activation of (pro)renin receptor promotes cell proliferation and tissue factor expression in vascular smooth muscle cells. *PLoS ONE* 9: e109268, 2014
28. Schulte TW, Blagosklonny MV, Romanova L, Mushinski JF, Monia BP, Johnston JF, Nguyen P, Trepel J, Neckers LM: Destabilization of Raf-1 by geldanamycin leads to disruption of the Raf-1-MEK-mitogen-activated protein kinase signalling pathway. *Mol Cell Biol* 16: 5839–5845, 1996
29. Grenert JP, Sullivan WP, Fadden P, Haystead TA, Clark J, Mimnaugh E, Krutzsch H, Ochel HJ, Schulte TW, Sausville E, Neckers LM, Toft DO: The amino-terminal domain of heat shock protein 90 (hsp90) that binds geldanamycin is an ATP/ADP switch domain that regulates hsp90 conformation. *J Biol Chem* 272: 23843–23850, 1997
30. Capodanno D, Angiolillo DJ: Antithrombotic therapy in patients with chronic kidney disease. *Circulation* 125: 2649–2661, 2012
31. Basra SS, Tsai P, Lakkis NM: Safety and efficacy of antiplatelet and antithrombotic therapy in acute coronary syndrome patients with chronic kidney disease. *J Am Coll Cardiol* 58: 2263–2269, 2011
32. Dember LM, Beck GJ, Allon M, Delmez JA, Dixon BS, Greenberg A, Himmelfarb J, Vazquez MA, Gassman JJ, Greene T, Radeva MK, Braden GL, Ikizler TA, Rocco MV, Davidson IJ, Kaufman JS, Meyers CM, Kusek JW, Feldman HI; Dialysis Access Consortium Study Group: Effect of clopidogrel on early failure of arteriovenous fistulas for hemodialysis: a randomized controlled trial. *JAMA* 299: 2164–2171, 2008
33. Crowther MA, Clase CM, Margetts PJ, Julian J, Lambert K, Sneath D, Nagai R, Wilson S, Ingram AJ: Low-intensity warfarin is ineffective for the prevention of PTFE graft failure in patients on hemodialysis: a randomized controlled trial. *J Am Soc Nephrol* 13: 2331–2337, 2002
34. Kolandaivelu K, Leiden BB, Edelman ER: Predicting response to endovascular therapies: dissecting the roles of local lesion complexity, systemic comorbidity, and clinical uncertainty. *J Biomech* 47: 908–921, 2014
35. Apetoh L, Quintana FJ, Pot C, Joller N, Xiao S, Kumar D, Burns EJ, Sherr DH, Weiner HL, Kuchroo VK: The aryl hydrocarbon receptor interacts with c-Maf to promote the differentiation of type 1 regulatory T cells induced by IL-27. *Nat Immunol* 11: 854–861, 2010
36. Quintana FJ, Sherr DH: Aryl hydrocarbon receptor control of adaptive immunity. *Pharmacol Rev* 65: 1148–1161, 2013
37. Kokubo T, Ishikawa N, Uchida H, Chasnoff SE, Xie X, Mathew S, Hruska KA, Choi ET: CKD accelerates development of neointimal hyperplasia in arteriovenous fistulas. *J Am Soc Nephrol* 20: 1236–1245, 2009
38. Itoh Y, Ezawa A, Kikuchi K, Tsuruta Y, Niwa T: Protein-bound uremic toxins in hemodialysis patients measured by liquid chromatography/tandem mass spectrometry and their effects on endothelial ROS production. *Anal Bioanal Chem* 403: 1841–1850, 2012
39. Niwa T: Targeting protein-bound uremic toxins in chronic kidney disease. *Expert Opin Ther Targets* 17: 1287–1301, 2013
40. Huang ST, Shu KH, Cheng CH, Wu MJ, Yu TM, Chuang YW, Chen CH: Serum total p-cresol and indoxyl sulfate correlated with stage of chronic kidney disease in renal transplant recipients. *Transplant Proc* 44: 621–624, 2012
41. Vanholder R, Schepers E, Pletinck A, Nagler EV, Glorieux G: The uremic toxicity of indoxyl sulfate and p-cresyl sulfate: a systematic review. *J Am Soc Nephrol* 25: 1897–1907, 2014

This article contains supplemental material online at http://jasn.asnjournals.org/lookup/suppl/doi:10.1681/ASN.2014121241/-/DCSupplemental.

Supplementary methods

Human subjects and serum collection

Uremic sera from patients of ESRD and control were pooled as described previously[8]. Briefly, the patients with ESRD on hemodialysis (HD) were recruited randomly from a pool of 150 patients at the DaVita Hemodialysis Center (Boston, MA). The protocol was approved both by Institutional Review Boards of Boston University Medical Center and Massachusetts Institute of Technology. Informed consents were obtained and 10 ml of blood collected prior to the next HD session. Patients with Hb <8 gm/dl were excluded. Control sera matched for age-, gender- and ethnicity-matched subjects were obtained from Research Blood Component Inc. (Boston, MA). The controls with creatinine more than 1.0 mg/dl were excluded.

LC/MS method validation

Linearity: IS standards in serum were linear in the range of 100 to 500,000 ng/ml during the LC-MS measurement. The linearity of IA and IS were 0.9998 and 0.9996, respectively (fig. S10B).

Lower Limit of Detectability (LLOQ**):** The concentration of IS in serum was diluted to 10, 20, 30, 40, 50, 100, 200, 300, 400, 500 ng/ml. Each sample was injected 6 times. The relative standard deviation was set at 15% for LLOQ. The LLOQ of serum IS is shown (Supplemental Figure 1).

Intra-assay and Inter-assay variation: Three spiked samples were used as quality controls. The value of 6 repeated injections in the same batch was used to calculate intra-assay variation. The samples analyzed in three different days were used to calculate inter-assay variation. The inter-assay and intra-assay variations were CV 5.4% and 0.9%, respectively (Supplemental table 2).

Recovery: Recovery describes the extraction efficiency of an analytical process, reported as a percentage of the known amount of an analyte carried through the sample extraction and processing steps. 400, 2000, 8000 ng/ml (final concentration) of IS was added to human serum. The measured concentration was used to calculate recovery. The recovery was 97-100% for IS (Supplemental table 3).

Lysis, immunoblotting, immunoprecipitation and immunofluorescence.

Cell harvest and immunoblotting have been previously described[8]. Monoclonal antibodies specific for tissue factor (Thermoscientific, HTF1), GAPDH (Cell signaling) and AHR, (Pierce-Thermoscientific) were used. The TF bands were normalized to GAPDH and quantified using ImageJ (NIH). Immunoprecipitation using tissue factor antibody (Thermoscientific, HTF1) or AHR antibody followed by agarose (A+G plus) beads (Santa Cruz) were performed as described previously [8]. The vSMCs grown in chamber slides (Lab-Tek) were fixed with methanol and processed as described previously using Leica SP5 confocal microscopy [8]. The MDA-MB231cells were transfected using Lipofectamine 2000 (Life Technologies). For IHC, polyclonal AHR-specific (Sanatcruz) and monoclonal TF-specific (Abcam) antibodies were used at a 1:50 dilution.

TF stability assay, ubiquitination assay

vSMCs treated with 20 μM Emetine for different time intervals were harvested for stability assay. The ubiquitination of TF was examined by pretreating vSMCs with proteasome inhibitor MG132 (Boston Biochem) at 10 μM for 6 hours followed by immunoprecipitation as described above. vSMCs cells lysates treated with uremic serum or solutes for 24 hours using 50 mM Tris buffered saline (pH 8.0) with 1% Triton X-100 and centrifuged at 14,000 g for 20 minutes.

RT-PCR

RNeasy mini kit (Qiagen) was used to extract total RNA from VSMCs. 300ng of total RNA were converted to cDNA using Sensiscript RT kit® (Qiagen) followed by RT-PCR using human TF, *Cyp1a1*, *Cyp1b1* and *Ahrr* primers (Qiagen) and SYBRgreen (Applied Biosystems). *Beta actin* served as a loading control. Levels of mRNA were determined using comparative Ct method.

vSMC injury scratch model:

One million vSMCs seeded on culture plates with 9 mm molded grid were treated with uremic solutes for 24 hours. The cells were then injured with a pipette tip by dragging along the grid. Cells were washed and incubated without uremic solutes for 2 hours prior to harvest.

Immunohistochemistry.

Paraffin-embedded tissue blocks of de-identified patients were processed after IRB approval. Tissue section preparation: Tissue blocks were cut into 7 µm thick tissue sections using a rotary microtome. The sections were allowed to float in a 56° C water bath. Tissue sections were mounted on pre-coated glass slides and dried overnight on heating block.

Immunostaining: Rehydration of the sections involved immersing them in xylene (two times) for 10 minutes each, followed by 100% ethanol (two times) for 3 minutes each, 95% ethanol for 1 minute, and 75% ethanol for 1 minute. The slides were rinsed with water and followed by heat-induced epitope retrieval along with citrate antigen retrieval buffer (ADI-950-270-0500). The slides were washed with distilled water and wiped around the sections to remove water. Tissue sections were marked using a hydrophobic

pencil followed by hydrogen peroxide block for 10 minutes. Further steps were carried out according to the manufacturer's instructions (Abcam-ab94709). AHR- (Santa Cruz SC-5579 and Tissue Factor-specific (Abcam-ab48647) antibodies were used.

Bacloviral protein production and *in vitro* binding assay:

A viral stock of human full length AHR was used to infect Sf9 cells, which were grown in Grace's medium containing 10% fetal bovine serum and 50 ug/ml gentamycin at 28^{o} C for 72 hours. The cells were harvested using Triton lysis buffer (1M Tris HCl, pH=7.6, 0.5M EDTA, 5M NaCl, triton X 100 and glycerol). After homogenization, the lysates were spun at 16000xg for 15 minutes at 4^{0} C. The supernatant was purified for overexpressed AHR using profanity IMAC Ni-charged resin (Biorad Cat #156-0131). The resin was washed with triton lysis buffer with 0.15, 0.2 and 0.3 M NaCl. Purified AHR protein was used in an *in vitro* binding assay with 1500 pM recombinant Tissue factor (HTI- RTI-300). Immunoblotting was performed as described previously (12, 49).

AHR Activity assay

AHR activity was examined in vSMCs using a promoter- reporter plasmid. The time of treatment with different reagents was optimized to obtain the best luciferase signal. vSMCs stably expressing Cignal Lenti Reporter xenobiotic response element tethered to luciferase reporter (XRE-luc) (Qiagen, CLS-9045L-8) seeded at 1000/well in 48 well plate were serum starved using 0.5% CS for 16 hours and treated with IS with or without AHR antagonist for 24 hours (Figure 1C). The firefly luciferase measured using luciferase assay kit (Promega# E1501) was converted to AHR activity using a standard curve generated with a canonical AHR agonist, FICZ (Supplemental Figure 6A).

The AHR activity in human serum was examined as described previously[41]. The optimum concentration of serum used for AHR assay was determined by treating with different percentages of sera for 4 hours (Supplementary Figure 4). HepG2 cells were

lyzed with passive lysis buffer and the luciferase activity was measured using luciferase assay kit (Promega# E1501) according to manufacturer's instructions, and the signal was normalized to protein. Serum of 1% yielded a maximum difference between control and uremic groups. Therefore, one percent serum concentration was selected to examine the AHR activity in individual ESRD sera samples.

TF procoagulant activity

TF surface/procoagulant activity was measured using a two-step FXa generation assay. A standard curve was generated by incubating human, recombinant lipidated TF (Enzolifesciences, Cat# SE-537) ranging from 0-500 pM along with 5nM of human factor VIIa (Enzyme Research Laboratories Cat# HFVIIa) and 150nM of factor X (Enzyme Research Laboratories Cat# HFX 1010) and CaCl2- 5mM for 30 minutes at 37^0C. The reaction mixture was incubated with chromogenic substrate for factor Xa (Chromogenix Cat# S2765, 1mM-final concentration). The reaction was stopped after 5 minutes using 10ul of 50% glacial acetic acid and read at 405nm absorbance. In vSMCs, the TF procoagulant activity was examined in 96 well plate format with 1000 vSMCs seeded per well. The cells were serum starved for 16 hours and treated with 1% sera for 24 hours. Cells were washed with TBS (50mM Tris HCl, 120mM NaCl, 2.7mM KCl, 3mg/ml BSA, pH=7.4) and incubated with 55ul TBS containing 5nM of human factor VIIa and 150nM of factor X and CaCl2- 5mM for 30 minutes at 37^0C. 50ul of the supernatant was incubated with chromogenic substrate at 1mM-final concentration. The reaction was stopped after 5 minutes by adding 10ul of 50% glacial acetic acid and the absorbance was read at 405nm. TF activity levels for samples were calculated using the regression analysis. To confirm the specificity of the TF activity assay, the TF activity was measured in the cells pre-treated with anti-TF neutralizing antibody (50ug/ml) or control for an hour, as described previously[8] (Supplemental Figure 2B). Platelet derived growth factor

(PDGF, R & D systems- cat# 220-BB-050) served as positive control (Supplemental Figure 2A).

Generation of CB7993113

CB7993113 was identified as an AHR antagonist and characterized as described[17].

Reagents.

Commercial chemical libraries of test compounds were acquired from ChemBridge Corporation and Enamine Ltd. Dimethyl sulfoxide (DMSO), b-Naphthoflavone (b-NF), 7,12-dimethylbenz[*a*]anthracene (DMBA), 2,3,7,8-tetrachlorodibenzo-*p*-dioxin (TCDD) and other chemical reagents were obtained from Sigma-Aldrich unless otherwise indicated. CB7993113 and CH223191 were synthesized as below. All compounds submitted for biological testing were deemed at least >98% pure by HPLC (with UV and mass spectral detection) and ^{1}HNMR. PDGF was obtained from R & D systems.

Chemical synthesis of 2-((2-(5-bromofuran-2-yl)-4-oxo-4H-chromen-3-yl)oxy)acetamide (CB7993113). 1-(2-hydroxyphenyl)ethanone (1.720 g, 14.29 mmol) and 5-bromofuran-2-carbaldehyde (2.5 g, 14.29 mmol) were dissolved in a round bottom flask in 10 mL of ethanol. Then, 1.5 mL of a solution of 17 M NaOH in water was added under vigorous stirring. Precipitate formed under addition of base and a thick paste was formed. The mixture was stirred for 24 hours at room temperature. Ethanol (50 mL) was added with 0.5 mL of 2.5 M NaOH. The mixture was cooled to 15° C and hydrogen peroxide was added (35% in water; 6.25 mL, 71.4 mmol). After 4 hours, dilute sulfuric acid was added to neutralize to pH 7.0 and the reaction was poured into 250 mL of water and stirred for 2 hours. The solid material was collected by filtration and dried under vacuum to give a yellow solid (1.01 g, 23% yield). ^{1}H NMR (399 MHz, DMSO-d_6) δ ppm 4.60 (s, 2 H) 6.98 (d, *J*=3.66 Hz, 1 H) 7.39 (br. s., 1 H) 7.50 (t, *J*=7.33 Hz, 1 H) 7.67 - 7.78 (m, 3 H) 7.81 (d, *J*=7.33 Hz, 1 H) 8.08 (d, *J*=8.06 Hz, 1 H).) A mixture of 2-(5-

bromofuran-2-yl)-3-hydroxy-4H-chromen-4-one, thus, obtained (910 mg, 2.96 mmol), 2-bromoacetamide (409 mg, 2.96 mmol), potassium carbonate (1229 mg, 8.89 mmol) and dimethylformamide (30 mL) were stirred for 6 hours at 80° C. The solution was cooled and extracted with ethyl acetate. The combined organic layers were washed with water, dried with sodium sulfate, filtered and concentrated. Toluene was added and evaporated repeatedly until dry crystals of crude product were formed. The resulting material was purified by column chromatography, first eluting impurities with 100% ethyl acetate, followed by 10% methanol in methylene chloride to provide CB7993113 as a yellow solid (900 mg, 83% yield). ^{1}H NMR (399 MHz, DMSO-d_6) δ ppm 4.60 (s, 2 H) 6.98 (d, *J*=3.66 Hz, 1 H) 7.39 (br. s., 1 H) 7.50 (t, *J*=7.33 Hz, 1 H) 7.67 - 7.78 (m, 3 H) 7.81 (d, *J*=7.33 Hz, 1 H) 8.08 (d, *J*=8.06 Hz, 1 H). (ESI) found 363.9 $[M + H]^{+}$.

Supplemental Figure 1. Development of LC/MS assay for IS measurement

A. Separation and detection of serum IS IS-d4. Separation was on Gemini C18 3µ column 50×2.0 mm Phenomenex. Analytes were eluted with a binary gradient consisting of solvent A (5 mmol/L ammonium acetate solution) and solvent B (methanol). The injection volume was 50 µL. (Insert) Fragmentation of IS. The fragment (M/Z 80.0) was the main fragment of IS. M/Z 212>80 was used for IS detection.

B. Linearity of IS on LC-MS/MS measurement. Known concentrations of IS were measured by above methods and correlation was performed using linear regression. Mean of two independent experiments is shown. Correlation coefficient was calculated using R^2.

C. Lower limit of quantitation (LLOQ). The concentration of IS in the spiked serum was diluted to 10,20,30,40,50,100,200,300,400 and 500 ng/ml. Each sample was injected 6 times and the relative standard deviation was calculated. Fifteen percent of relative standard deviation was set as LLOQ. The LLOQ of serum IS was 20 ng/ml.

Supplemental Figure 2. Development and validation of procoagulant TF activity assay in vSMCs.

A. Increase in procoagulant TF activity in vSMCs by PDGF. Dynamic range of the procoagulant TF activity assay was determined using PDGF, a known inducer of TF activity[9]. Serum starved vSMCs were incubated with various concentration PDGF for 24 hours. An average of three independent experiments is shown. Error bars = SD. Compared to control, p = 0.02 for PDGF of 10 ng/ml, p = 0.004 of 20 ng/ml, p = 0.001 of 30 ng/ml, p = 0.03 of 40 ng/ml.

B. Specificity of procoagulant TF activity assay. Serum starved vSMCs were treated with 5% pooled control or uremic serum control or anti-TF neutralizing antibody for 24 hours, as described previously[8] and the procoagulant TF activity assay was performed.

An average of three independent experiments is shown. Error bars = SD. Compared to control serum, p = 0.001 for uremic serum. In the both groups, the anti-TF neutralizing antibody significantly suppressed the TF activity, p = 0.01 in the control serum group, and p = 0.004 in the uremic serum group.

Supplemental Figure 3. AHR and TF expression in human blood vessels

A. Expression of AHR in vascular smooth muscle (vSMCs) in human interlobular renal artery. Paraffin-embedded sections of renal artery of a 51-year-old female were stained for isotype control IgG or AHR antibodies. A representative image from five independent patient samples is shown. Images were captured at 20X magnification. Atherosclerotic plaque with intimal vSMC is shown. EC= endothelial cells, vSMCs = vascular smooth muscle cells. The yellow arrow shows the fragmented internal elastic lamina. Scale bar = 100 µM

B. Expressions of TF and AHR in vSMCs in subcutaneous arterioles obtained from below knee-amputated limb. Paraffin-embedded sections from the amputated limb of a 79-year-old diabetic and hypertensive patient were stained for TF or AHR or isotype control antibodies. A representative image from three independent patient samples is shown. Images were captured at 20X magnification. The yellow arrow shows an integrated thrombus within the vessel wall. Scale bar = 100 µM

Supplemental Figure 4. AHR activity assay for human serum

We first determined the optimum concentration of human serum to be used for AHR activity by exposing serum starved cells stably expressing Cignal Lenti Reporter (XRE-luc) to different concentrations of pooled control or uremic sera for 4 hours [41]. AHR antagonist CH223191- 10 µM served as a negative control. The luciferase reading was normalized for protein content. An average of three different experiments performed in

duplicate is shown. One percent serum yielded highest difference between two groups (5.7 relative luciferase unit per µg protein, p = 0.001). Therefore, one percent serum concentration was selected to examine the AHR activity in individual ESRD sera samples as shown in Table 2. Error bars = SD. Compared to the control group, uremic group had following p values. p = 0.002 0.001% serum, p = 0.002 for 0.1% serum and p = 0.001 for 1% serum. Compared to vehicle treated cells, p = 0.01 in control serum and p = 0.0001 in uremic serum treated with 10 µM of AHR antagonist.

Supplemental Figure 5. Molecular structure of AHR antagonist

A. Structures of CB7993113 2-{[2-(5-bromo-2-furyl)-4-oxo-4H-chromen-3-yl]oxy}acetamide

B. Structures of CH223191 (E)-1-Methyl-N-(2-methyl-4-(o-tolyldiazenyl)phenyl)-1H-pyrazole-5-carboxamide

Supplemental Figure 6. AHR unit determination and bound form of IS induces AHR activity in an AHR-dependent manner

A. AHR activity unit determination. Primary aortic vSMCs stably expressing a dioxin responsive element (DRE) promoter-luciferase reporter construct were treated with indicated concentrations of FICZ for 24 hours in serum free medium. AHR activity was quantified by firefly luciferase units measured using luciferase assay kit (Promega# E1501) normalized to protein concentration. An average of three independent experiments is shown. Compared to control, p values for different FICZ concentrations were p = 0.042 for 1 ng/ml, p = 0.004 for 10 and 20 and 40 ng/ml of FICZ, and 0.001 for more than 60 ng/ml FICZ. Error bars = SD. The linear regression was applied to obtain the equation and R^2 value.

B. Bound form of IS corresponding to the levels in different stages of CKD induces AHR activity. vSMCs stably expressing xenobiotic responsive element (XRE) promoter-luciferase reporter construct were treated with different concentrations of IS or human serum albumin (Ctr) for 24 hours and the firefly luciferase measured as above was converted to AHR activity units using the standard curve generated with FICZ, a canonical AHR agonist (Supplemental Figure 6A). Mean result of three experiments is shown. Error bars = SD. Compared to the control (HSA) IS μg/ml, $p = 0.01$ for IS 5 μg/ml, $p = 0.001$ for IS 10, 15, 20 μg/ml and $p = 0.008$ for IS 40 μg/ml.

C. AHR antagonist inhibits AHR activity induced by bound form of IS. vSMCs stably expressing xenobiotic responsive element (XRE) promoter-luciferase reporter construct were treated with IS or human serum albumin (HSA) and different concentration of CB7993113 for 24 hours and the firefly luciferase was converted to AHR activity units as mentioned above. Mean result of three experiments is shown. Error bars = SD. Compared to IS alone, the IS + CB7993113 treated cells, $p = 0.05$ for 5 μM, $p = 0.002$ for 10, 20 μM and $p = 0.001$ for 30 and 40 μM.

Supplemental Figure 7. Wild-type mouse embryonic fibroblasts (MEFs) have higher TF compared to AHR KO MEFs; and modulation of TF by known AHR ligands

A. AHR KO MEFs have lower TF compared to wild-type MEFs. MEFs from C57BL/6 animals and AHR KO animal on the same background were lyzed and probed for TF. GAPDH served as loading control. A representative of 2 independent experiments is shown.

B. Regulation of TF by known AHR ligands. Primary aortic vSMCs at passage 6 were treated with AHR ligands (**B**) AHR agonists- 6-formylindole[3,2-b]carbazole (FICZ) (**C**) and β-naphtoflavone (β-NF) and (**D**) an AHR antagonist, 3'methoxy-4'nitroflavone (MNF)

in the concentration as shown for 24 hours. The lysates were probed for TF and GAPDH, where served as a loading control. TF bands were normalized by GAPDH. Representative figure from three independent experiments is shown.

Supplemental Figure 8. Rise in TF mRNA follows the effect on protein levels with IS treatment

TF mRNA increases after 4 hours of IS treatment. vSMCs treated with IS (25 µg/ml) or control were harvested at indicated time intervals. Quantitative RT-PCR in two steps was performed after extracting RNA and synthesizing cDNA using random hexamers and oligo dT primers. qRT-PCR reactions were processed in duplicate for each sample and quantified using real time PCR for detecting TF mRNA. The Ct values were utilized to generate delta-delta ct values normalized by GAPDH levels. An average from three independent experiments is shown. Error bar = SD. p = 0.008 for TF mRNA after 4 hours.

Supplemental Figure 9. TF half-life reduced with AHR antagonist

A. AHR antagonist destabilizes TF at baseline. vSMCs treated with CB7993113 10 µM for 24 hours were treated with Emetine 20 µM and harvested at indicated time for TF expression. A representative blot from three experiments is shown. For all the blots, the values below the blot represents the normalized bands against GAPDH using ImageJ.

B. Densitometry was performed on half-life study using Image J and GAPDH was used to normalize the TF signal. Average of three experiments is shown. Error bars = SD. Compared to TF in control, p = 0.05 at 0.5 hours, p = 0.01 at 1 hour and p = 0.002 at 4 hours in CB7993113 treated cells.

Supplemental Figure 10. IS corresponding to the levels seen in early stages of CKD increase TF expression and activity in vSMCs

A. IS levels corresponding to different stages of CKD increase TF expression. Lysates of vSMCs treated with IS or control at different concentrations were resolved on SDS page gel and immunoblotted with TF antibody. GAPDH served as loading control. Average IS levels found in the patients with different stages of CKD is shown in Supplementary table S3. A representative of three independent experiments is shown.

B. IS levels corresponding to different stages of CKD increase procoagulant TF activity. TF activity was examined in vSMCs exposed to IS levels corresponding to different stages of CKD as shown in supplementary table S3. An average of three experiments is shown. Error bars = SD. Compared to control, $p = 0.02$ for IS 1µM, $p = 0.001$ for IS 10µM, $p = 0.003$ for IS 10µM.

Supplemental Table 1. ESRD patient characteristics

No	Age	Sex	Ethnicity	Cause	DM	HTN	BMI	SBP	DBP	Hb	Platelet	INR	Chol	LDL	Epogen	sp KT/V
1	60	M	AA	DM+HTN	1	1	38	182	89	8.9	246	0.87	100	54	9900	1.36
2	27	F	AA	HTN	0	1	30.6	156	82	8.6	295	1.00	245	161	12000	1.23
3	40	F	AA	Collapsing GN	0	1	40.58	174	93	9.2	232	0.99	170	74	8525	1.95
4	51	M	AA	Collapsing GN	0	1	24	182	86	11	257	1.00	283	183	39600	1.1
5	73	M	AA	DM+HTN	1	1	33.25	187	100	10.8	85	2.60	106	56	15400	1.6
6	41	M	AA	HTN	0	1	22.9	132	84	9.2	242	1.30	84	38	6600	1.05
8	52	F	HIPS	HTN	0	1	41.46	162	94	12	305	0.97	232	141	23870	1.25
9	33	M	AA	HTN	0	1	25.2	158	86	13.2	208	0.96	141	71	57490	1.7
10	57	M	AA	DM	1	1	17.6	152	90	10.7	172	1.20	88	52	20500	1.73
11	56	M	HISP	DM	1	1	28.7	162	96	10.8	143	0.97	195	132	18000	1.39
12	70	M	AA	DM+HTN	1	1	24.1	150	88	12	232	0.95	116	64	15000	1.05
13	36	F	HISP	SLE	0	0	18.7	93	68	12.1	120	1.70	176	115	NA	1.99
14	50	M	AA	HTN	0	1	21.8	150	85	11.6	188	0.96	170	85	NA	1.4
15	55	M	AA	DM+HTN	1	1	32.61	140	96	8.6	207	1.18	181	114	19800	1.66
16	52	M	ASIAN	DM	1	1	22.3	139	88	9.3	198	0.96	161	78	6600	1.76
17	46	M	AA	DM+HTN	1	1	27.09	152	92	9.9	178	0.96	145	87	NA	1.67
18	28	M	AA	HTN	0	1	26.27	142	96	10.8	247	0.88	231	146	39600	1.79
19	29	M	AA	Reflux Neph	0	1	24	178	102	12.3	220	0.88	NA	NA	NA	1.67
20	47	F	AA	FSGS	0	1	26	156	110	9.6	242	1.05	86	20	19800	1.25
21	48	M	AA	DM+HTN	1	1	31.3	128	86	9.2	210	0.96	195	113	NA	1.11

AA= African American, Hispan = Hispanic, DM= diabetes, HTN= hypertension, Reflux Neph = reflux nephropathy, SLE = systemic lupus erythematosus, GN = glomerulonephritis, 0 = absent, 1= present, BMI= kg/m2, SBP= systolic blood pressure mm Hg, DBP= diastolic blood pressure mm Hg, Platelet is K/ul, Chol = total cholesterol mg/dl, LDL = LDL cholesterol mg/dl, Epogen = unit/week, spKt/v= single pool Kt/V and NA= not available.

Supplemental Table 2. Inter assay and intra-assay variability of estimation of IS

Intra-assay Variation			
	Average	SD	CV (%)
QC1	236	14	5.8
QC2	377	29	7.7
QC3	4939	279	6
Inter-assay Variation			
	QC1	QC2	QC3
Assay 1	236	377	4939
Assay 2	259	424	4977
Assay 3	220	376	4889
Average	238	392	4935
SD	20	27	44
CV(%)	8.2	7.0	0.9

Supplemental Table 3. Recovery of IS sample

	Orogonal		Add 400 ng/ml			Add 2000 ng/ml			Add 80000 ng/ml	
	Conc ng/ml		Conc ng/ml	Recovery (%)		Conc ng/ml	Recovery (%)		Conc	Recovery (%)
Serum	376±29		831±35	113.7		2631±102	112.7		8988±402	107.6

Supplemental Table 4. Levels of IS in different stages of CKD[24, 37-39]

	eGFR ml/min	Average total IS µg/ml	Average total IS µM*	**Expected Free IS (µg/ml)
Normal	>90	0.243	0.97	0.02
Stage I**	>90	0.243	0.97	0.02
Stage II	60-89	0.5	1.98	0.05
Stage III	30-59	3.2	12.73	0.32
Stage IV	15-29	5.4	21.48	0.54
Stage V	<15	19.8	78.79	1.98
ESRD	<15HD	44.86	169.12	4.25

eGFR = estimated Glomerular filtration rate, mg/dL = milligram / 100 ml
*Calculated based on formula weight of IS = 251.30
**Free form of IS calculated as 10% of total IS

Supplemental Table 5. Levels of IS and AHR and TF activities in non-diabetic ESRD patients matched with controls

Pairs	IS µg/ml		AHR activity RLU/ug		TF activity pM	
	Control	Uremic	Control	Uremic	Control	Uremic
1.00	0.65	21.85	1.82	4.21	206.62	271.90
2.00	1.30	48.85	2.00	5.48	149.75	297.93
3.00	1.33	24.75	1.39	3.50	247.96	284.50
4.00	0.08	70.50	2.30	7.60	185.93	319.83
5.00	0.33	26.75	1.98	5.52	234.44	284.79
6.00	2.40	52.65	1.91	3.02	316.00	426.32
7.00	0.43	11.10	1.49	3.62	286.43	276.63
8.00	1.39	58.40	2.38	5.99	192.66	330.10
9.00	0.85	73.25	1.91	5.76	128.19	428.42
10.00	1.22	44.65	1.88	5.31	218.04	276.63
11.00	1.47	13.95	1.91	4.38	187.73	274.24
Mean	1.04	40.61	1.91	4.94	213.98	315.57
Median	1.22	44.65	1.91	5.31	206.62	284.79
SD	0.66	22.09	0.29	1.34	55.42	58.40

Supplemental Table 6. Comparision of controls and non-diabetic ESRD patients

	Paired T	Wilcoxon Signed-Rank
IS levels µg/ml	0.0001	0.001
AHR activity RLU/ug	<0.0001	0.001
TF activity pM	0.0021	0.002

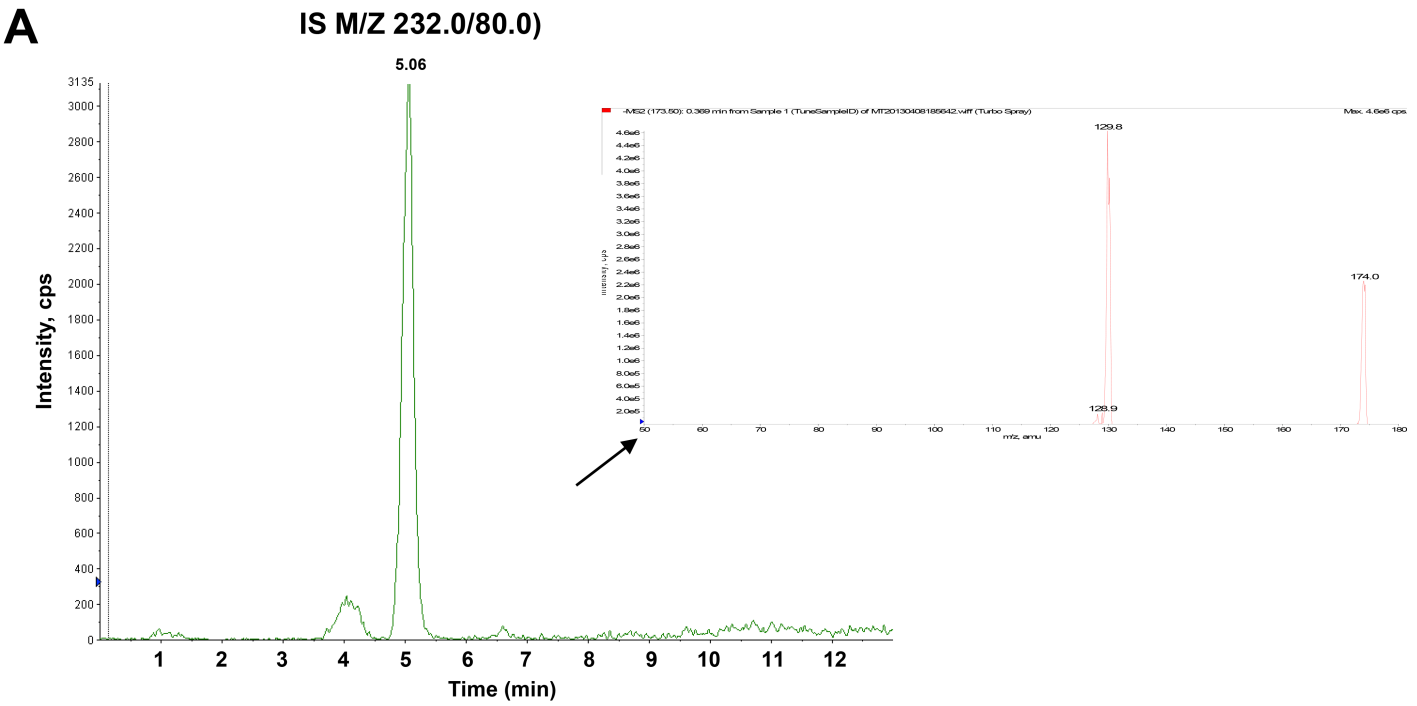
A
IS M/Z 232.0/80.0)
5.06
Intensity, cps
Time (min)
129.8
174.0
129.9
B
0618 validation 1 .rdb (IS): "Linear" Regression ("NO" weighting): y=0.00347 x + 0.0533 (r=0.9996)
Analyte Area / IS Area
Analyte Conc. / IS Conc.
C
Lower Limit of Quantitation of Plasma Indoxyl Sulfate
Relative Standard Deviation (%)
Concentration of Plasma Sulfate (ng/ml)

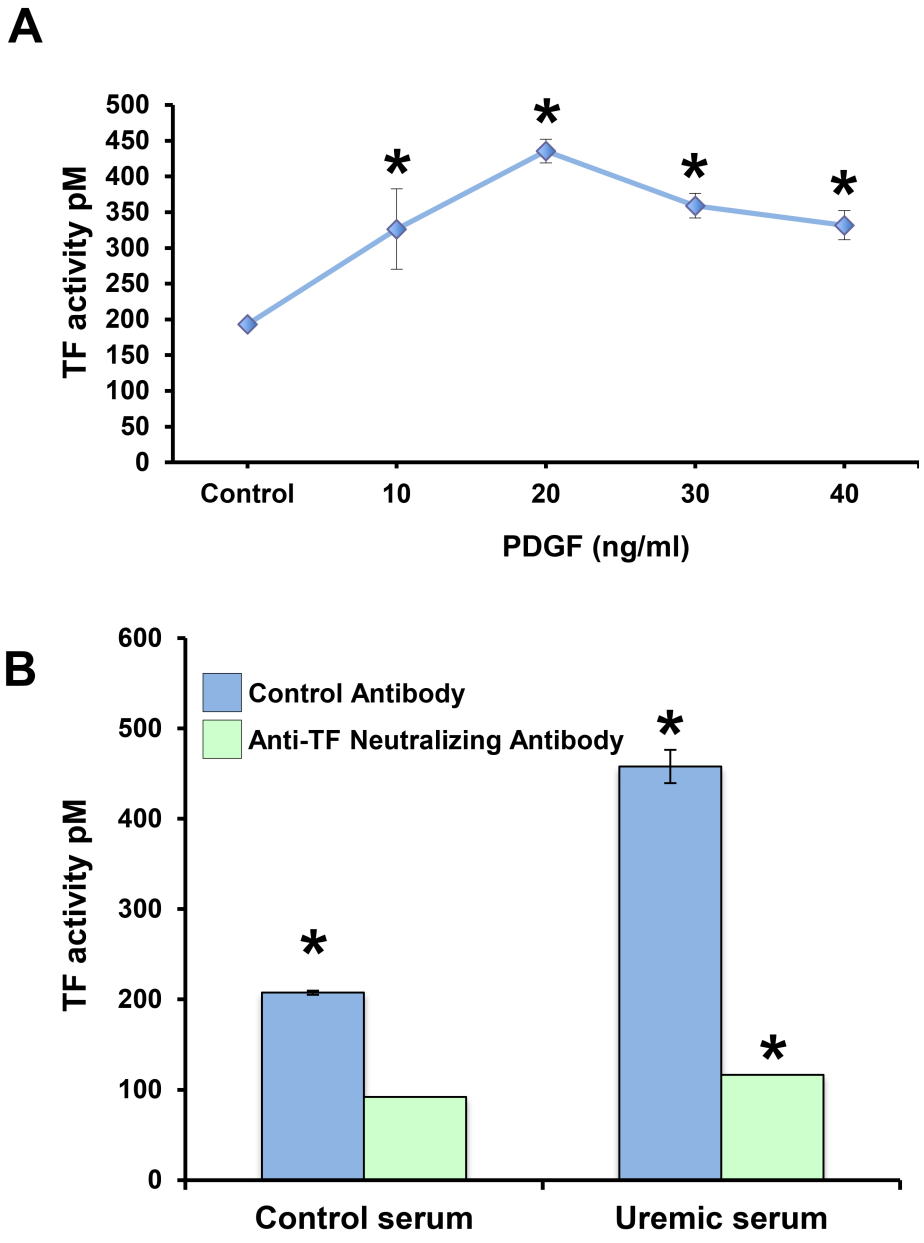
A
TF activity pM
500
450
400
350
300
250
200
150
100
50
0
Control
10
20
30
40
PDGF (ng/ml)
*
*
*
*
B
TF activity pM
600
500
400
300
200
100
0
Control Antibody
Anti-TF Neutralizing Antibody
Control serum
Uremic serum
*
*
*

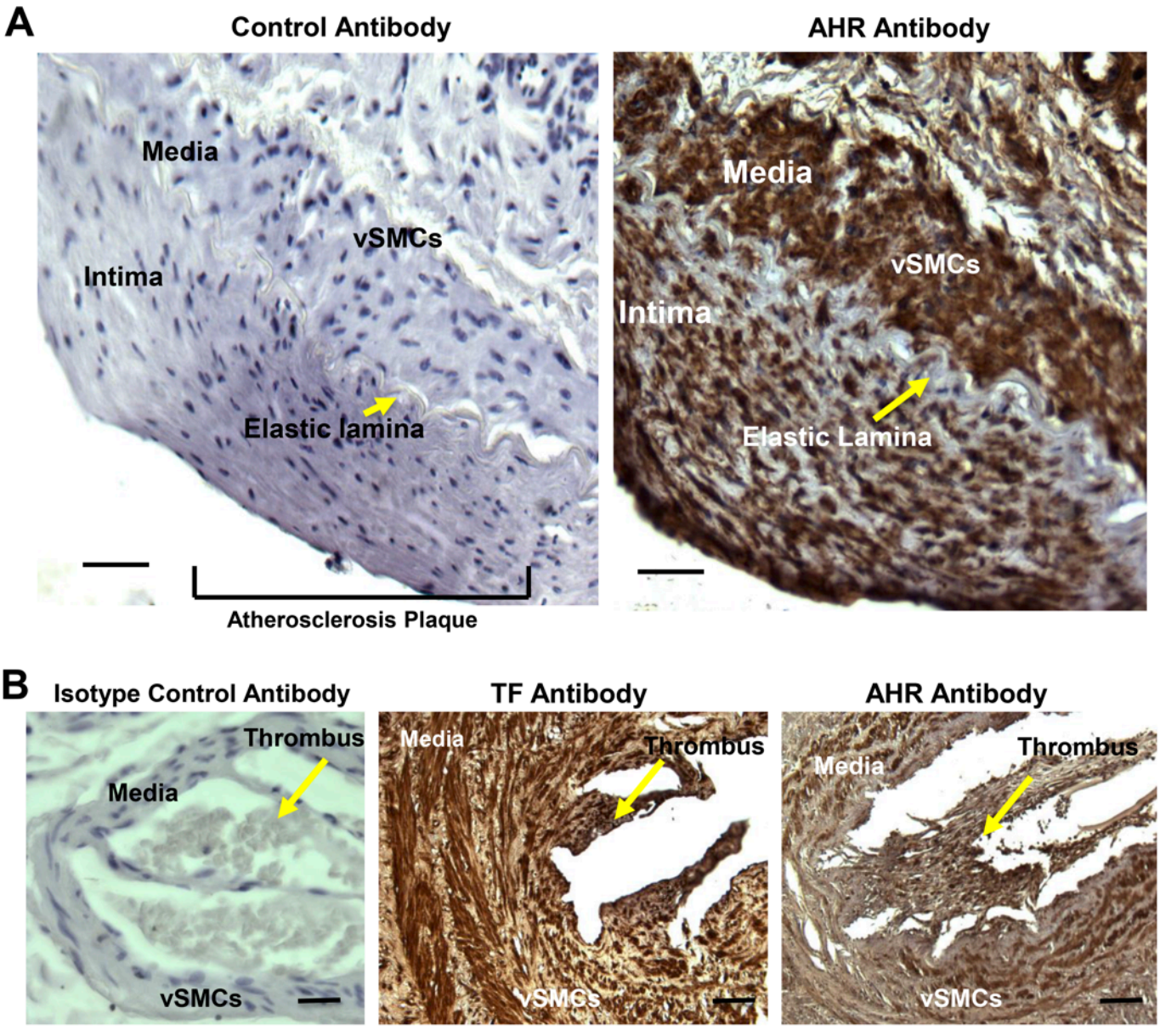
A
Control Antibody
AHR Antibody
Media
vSMCs
Intima
Elastic lamina
Media
vSMCs
Intima
Elastic Lamina
Atherosclerosis Plaque
B
Isotype Control Antibody
TF Antibody
AHR Antibody
Thrombus
Media
vSMCs
Media
Thrombus
vSMCs
Media
Thrombus
vSMCs

Supplementary Figure 4

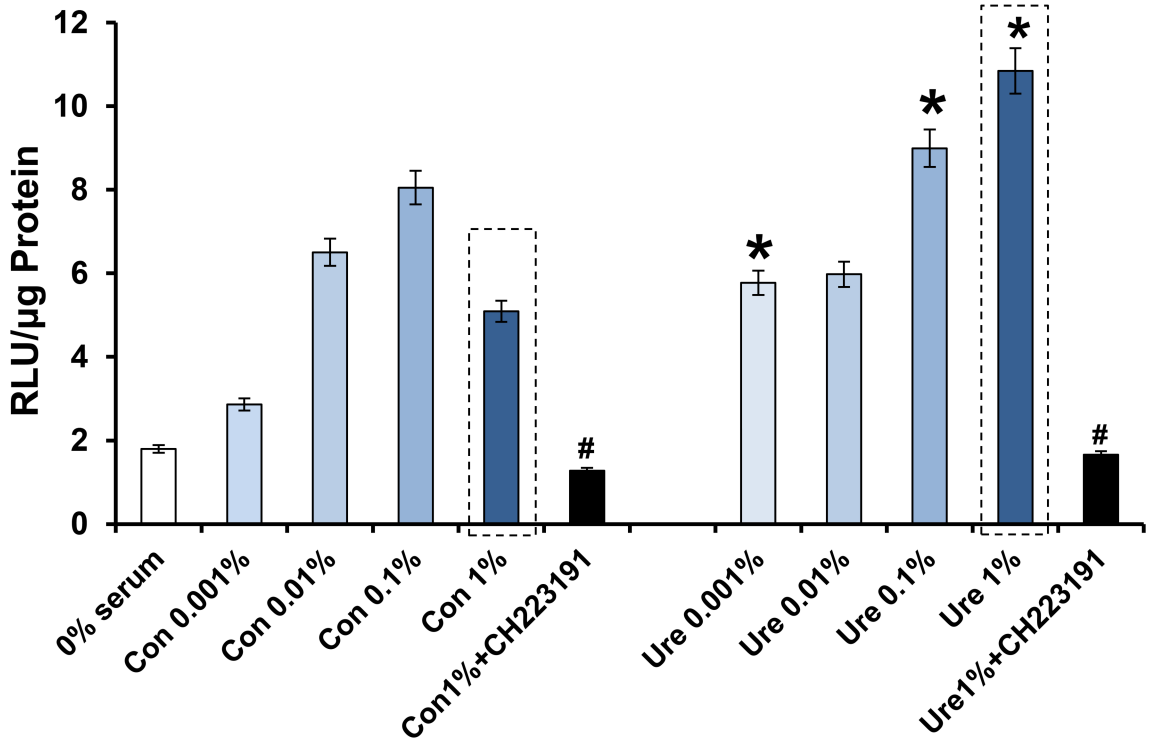

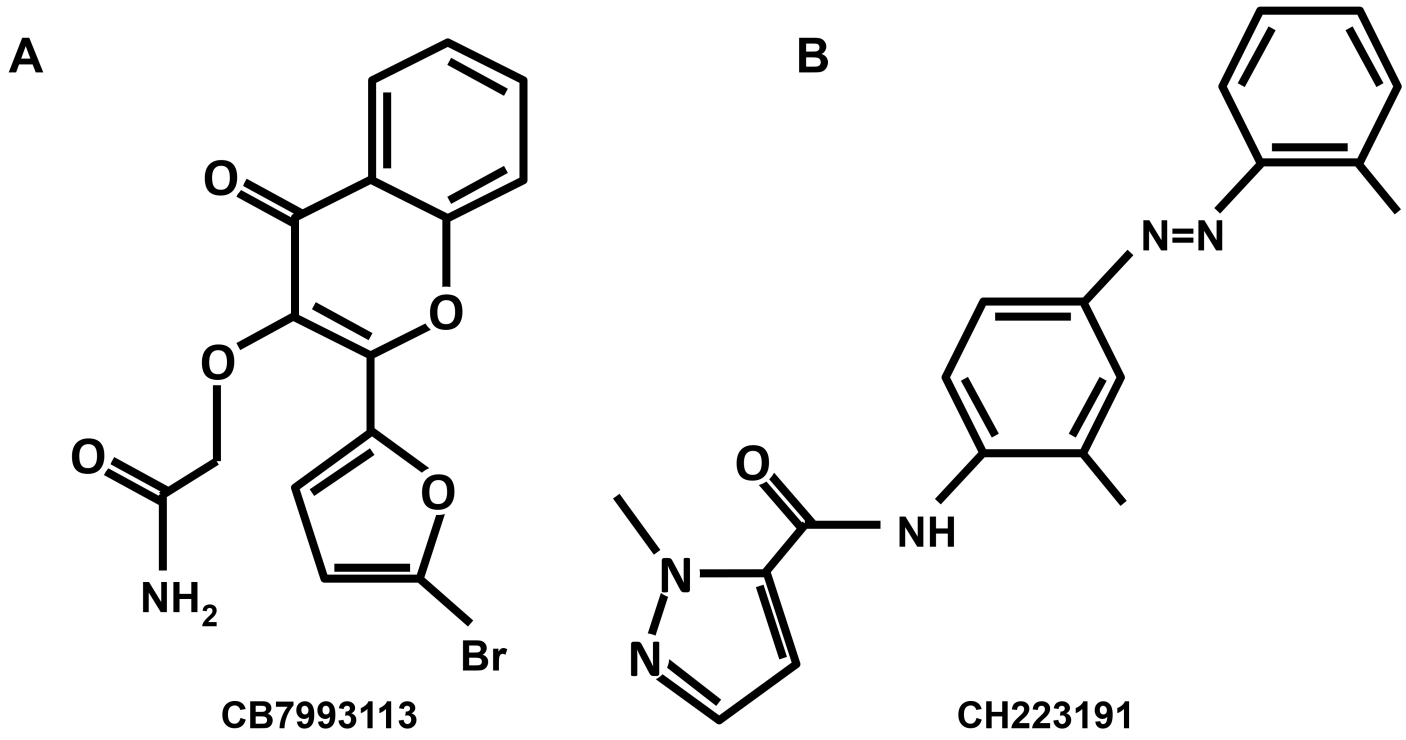
A
O
O
O
O
O
NH2
Br
CB7993113
B
N=N
O
NH
N
N
CH223191

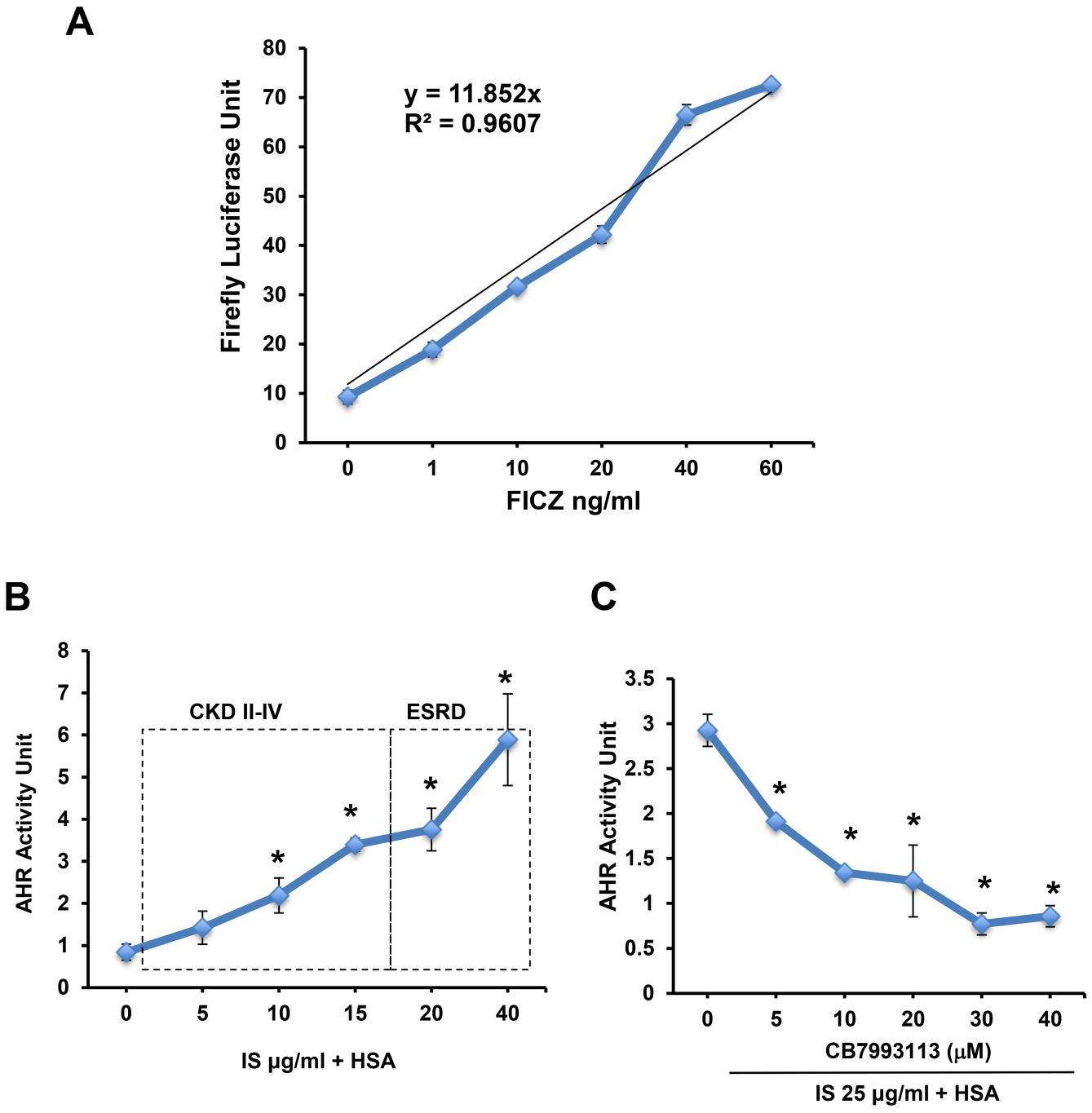
A
y = 11.852x
R² = 0.9607
Firefly Luciferase Unit
FICZ ng/ml
B
CKD II-IV
ESRD
AHR Activity Unit
IS μg/ml + HSA
C
AHR Activity Unit
CB7993113 (μM)
IS 25 μg/ml + HSA

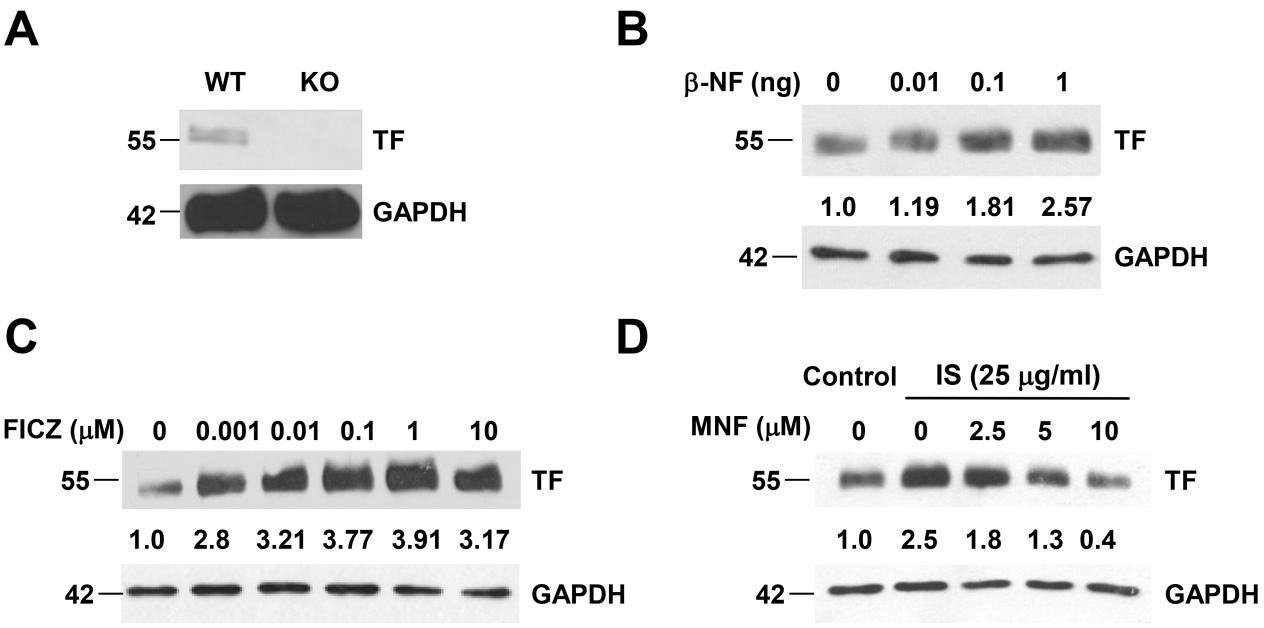
A
WT
KO
55
TF
42
GAPDH
B
β-NF (ng) 0 0.01 0.1 1
55
TF
1.0 1.19 1.81 2.57
42
GAPDH
C
FICZ (μM) 0 0.001 0.01 0.1 1 10
55
TF
1.0 2.8 3.21 3.77 3.91 3.17
42
GAPDH
D
Control
IS (25 μg/ml)
MNF (μM) 0 0 2.5 5 10
55
TF
1.0 2.5 1.8 1.3 0.4
42
GAPDH

Supplementary Figure 8

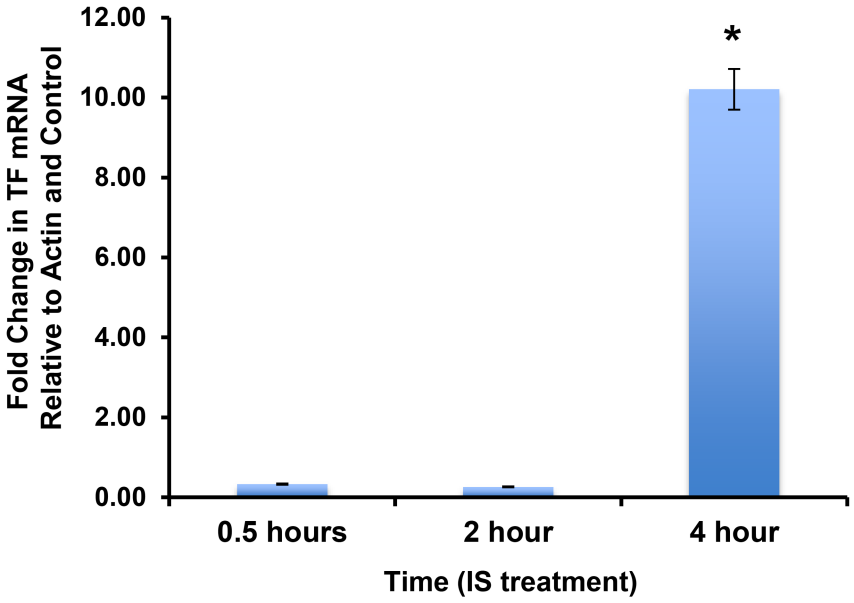

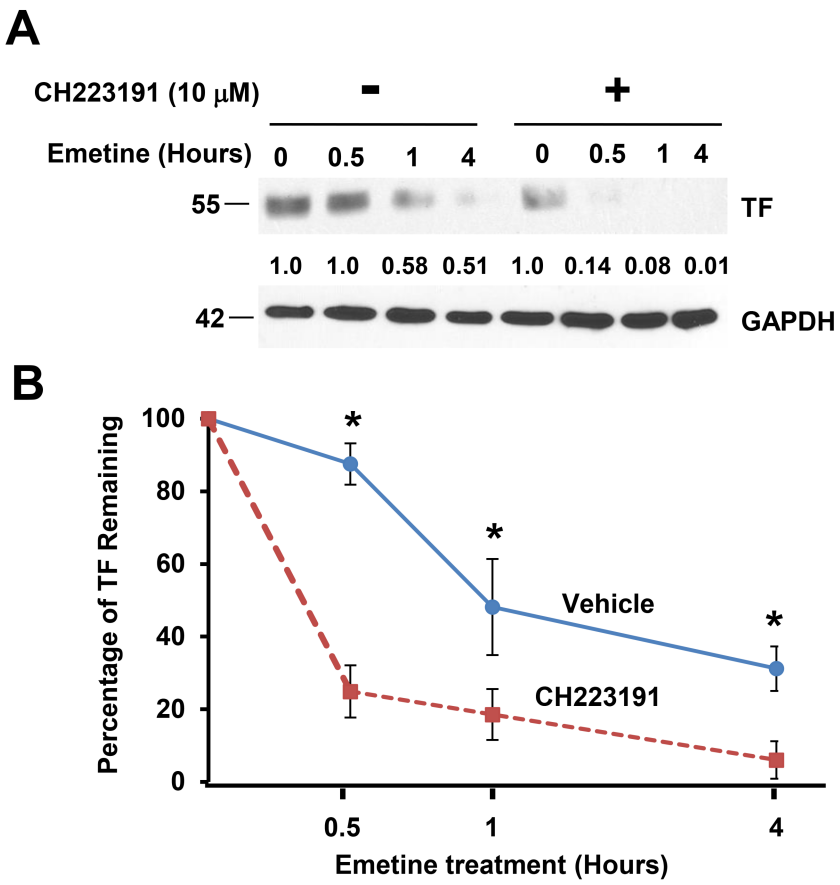
A
CH223191 (10 μM)
-
+
Emetine (Hours)
0
0.5
1
4
0
0.5
1
4
55
TF
1.0
1.0
0.58
0.51
1.0
0.14
0.08
0.01
42
GAPDH
B
Percentage of TF Remaining
100
80
60
40
20
0
*
*
*
Vehicle
CH223191
0.5
1
4
Emetine treatment (Hours)

Supplementary Figure 10